

# The Araucaria Project: VLT-spectroscopy of blue massive stars in NGC 55<sup>★</sup>

N. Castro<sup>1,2</sup>, A. Herrero<sup>1,2</sup>, M. Garcia<sup>1</sup>, C. Trundle<sup>3</sup>, F. Bresolin<sup>4</sup>, W. Gieren<sup>5</sup>,  
G. Pietrzyński<sup>5,6</sup>, R. -P. Kudritzki<sup>4</sup>, and R. Demarco<sup>7</sup>

<sup>1</sup> Instituto de Astrofísica de Canarias, C/ Vía Láctea s/n, E-38200 La Laguna, Tenerife, Spain.

<sup>2</sup> Departamento de Astrofísica, Universidad de La Laguna, Avda. Astrofísico Francisco Sánchez s/n, E-38071 La Laguna, Tenerife, Spain.

<sup>3</sup> Astronomy Research Centre, Department of Physics & Astronomy, School of Mathematics & Physics, The Queen's University of Belfast, Belfast, Northern Ireland, UK.

<sup>4</sup> Institute for Astronomy, 2680 Woodlawn Drive, Honolulu, HI 96822, USA.

<sup>5</sup> Departamento de Física, Astronomy Group, Universidad de Concepción, Casilla 160-C, Concepción, Chile.

<sup>6</sup> Warsaw University Observatory, Al. Ujazdowskie 4,00-478, Warsaw, Poland.

<sup>7</sup> Department of Physics and Astronomy, The Johns Hopkins University, Baltimore, MD 21218, USA.

Received January 15, 2008; accepted March 31, 2008

## ABSTRACT

**Aims.** This is the first paper of a series devoted to studying the population of blue massive stars in NGC 55, a galaxy of the Sculptor group at a distance of about 2 Mpc.

**Methods.** We have obtained optical (3300–6210Å), low-resolution spectra of approximately 200 blue massive stars with VLT-FORS2, which we have classified with the aid of Milky Way and Magellanic Cloud standard stars.

**Results.** We present the first census of massive blue stars in NGC 55. A study of stellar radial velocities shows agreement with existing HI rotational velocity curve work and reveals the presence of one object with peculiar velocity. A qualitative study of the stellar metallicity suggests that its global distribution over NGC 55 is close to that of the LMC, as derived from previous studies.

**Conclusions.** We present a catalogue with 164 classifications of blue massive stars in NGC 55. This catalogue is a first and necessary step for the subsequent quantitative study of blue massive stars in NGC 55 with state-of-the-art model atmospheres.

**Key words.** Galaxies: individual: NGC 55 – Galaxies: stellar content – Stars: early-type – Stars: fundamental parameters – Catalogs.

## 1. INTRODUCTION

The exploration of massive stars in nearby galaxies is experiencing a renewed interest since it became possible to study them spectroscopically outside the Milky Way, even beyond the Local Group, with the new generation of 8-10m class telescopes. There are many reasons for our interest in massive stars: they are the main source of ionisation and chemical enrichment of the Universe and their influence on the chemical and dynamical evolution of galaxies is very strong due to their stellar winds and supernova explosions. Additionally, blue massive stars can be used to measure distance by means of the relationship between their luminosity and their wind momentum (Kudritzki et al. 1995) or their flux-weighted gravity  $g/T_{eff}^4$  (Kudritzki et al. 2003, 2008). Once calibrated, these techniques can provide distance estimates to the Virgo and Fornax clusters as an alternative distance diagnostic to Cepheids, and with comparable accuracy (see Kudritzki et al. 1999 and references above). However, our knowledge of massive stars is incomplete and the physics involved in their formation and evolution is not totally understood (Kudritzki & Puls 2000; Massey 2003).

Modelling the atmospheres of these stars is a complex task involving non-local thermodynamical equilibrium processes,

and strong stellar winds in a spherically extended atmosphere. Each atmospheric model is computed with several free parameters, all of which have different effects on the emerging spectrum. The stellar metal content is crucial, since the stellar wind is driven by the moment transfer between photons escaping from the photosphere and metallic ions (Kudritzki & Puls 2000). Beyond the Milky Way we can study the impact of metallicity on stellar properties, evolution and feedback. Consequently, there is growing interest in studies of massive stars in galaxies with different metal content. In our Galaxy there are numerous studies of clusters and associations (Herrero et al. 1999; Rolleston et al. 2000; Smartt et al. 2001; Herrero et al. 2002; Daflon & Cunha 2004; Dufton et al. 2006), but the Magellanic Clouds are the most targeted due to their proximity and their different metallicity from the Milky Way (Lennon et al. 2003; Rolleston et al. 2003; Trundle et al. 2004; Korn et al. 2005; Lennon et al. 2005; Trundle & Lennon 2005; Hunter et al. 2007; Mokiem et al. 2007; Trundle et al. 2007). Additional work on other galaxies of the Local Group include: M 31 (Venn et al. 2000; Trundle et al. 2002), M 33 (Monteverde & Herrero 1998; Monteverde et al. 2000; Urbaneja et al. 2005b), NGC 6822 (Musciellok et al. 1999; Venn et al. 2001), NGC 3109 (Evans et al. 2007), WLM (Venn et al. 2003; Bresolin et al. 2006) or IC 1613 (Bresolin et al. 2007). Detailed quantitative analyses of extragalactic massive stars reach as far as NGC 300 in the Sculptor group (Bresolin et al. 2002a; Urbaneja et al. 2005a) where iron-group elements

Send offprint requests to: N. Castro (e-mail: norberto@iac.es)

<sup>★</sup> Based on observations obtained at the ESO VLT for Large Programme 171.D-0004.

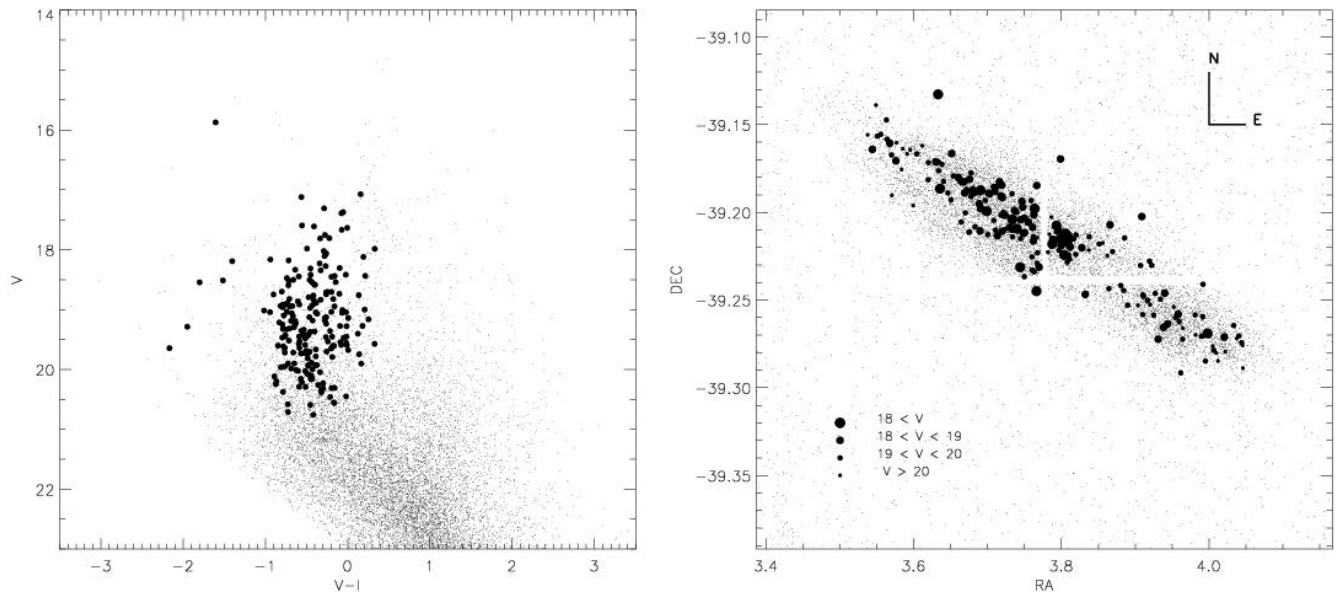


**Fig. 1.** Left: Colour-magnitude diagram of NGC 55. The targets selected for the spectroscopic study presented in this paper are marked with circles. Right: Location of the target stars in NGC 55. Note that they are spread across the galaxy providing information from different points of NGC 55.

have been studied for the first time outside the Local Group by Kudritzki et al. (2008). Beyond that, Bresolin et al. (2001) managed to determine global metallicities for A-type supergiants in NGC 3621 at a distance of 6.7 Mpc.

We now extend the study of massive extragalactic stars to NGC 55. This galaxy is located in the Sculptor group at 1.94 Mpc (Pietrzyński et al. 2006; Gieren et al. 2008), close enough to allow quantitative spectroscopic analyses of bright blue stars. Its large inclination angle ( $\sim 80^\circ$ , Hummel et al. 1986) makes its morphological classification difficult. Some authors argue that NGC 55 is a Magellanic irregular (see for instance Davidge 2005), however we adopt de Vaucouleurs (1961)’s SB(s)m classification for this work. It is one of the largest galaxies of the Sculptor group, together with NGC 300 and NGC 247, and its chemical composition is similar to that of the Large Magellanic Cloud (LMC) ( $[\text{Fe}/\text{H}] \sim -0.3$ , Davidge 2005). Photometric studies hint an important population of blue stars (Gieren et al. 2005) mainly in the central region, where intense stellar activity is revealed by bubbles and filaments produced by strong stellar winds and supernova explosions (Tüllmann et al. 2003).

In this paper the first study and census of massive blue stars in NGC 55 is presented. In section 2 we describe briefly the target selection process, the observations and the data reduction. In section 3 we discuss the spectral classification criteria for our catalogue of blue stars in NGC 55. We provide rough estimates for the distribution of stellar radial velocities and metallicities in sections 4 and 5. Finally, a summary and our conclusions are presented in section 6.

## 2. OBSERVATIONS AND DATA REDUCTION

Targets were selected from existing V- and I-band photometry obtained as part of the ongoing ARAUCARIA Cepheid search project<sup>1</sup> whose results have been reported in Pietrzyński et al. (2006). These data were taken with the Warsaw 1.3 m telescope

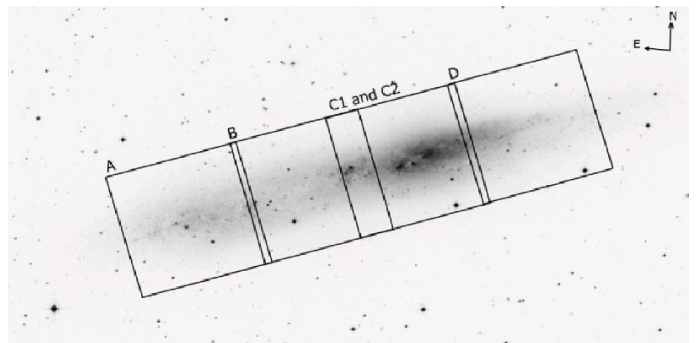


**Fig. 2.** Observed fields of NGC 55. Each square represents approximately the FORS2 field of view ( $6'.8 \times 6'.8$ ) in MXU mode. The image was taken from the DSS archive ([http://archive.stsci.edu/cgi-bin/dss\\_form](http://archive.stsci.edu/cgi-bin/dss_form)).

at Las Campanas Observatory. The telescope is equipped with a mosaic CCD  $8k \times 8k$  with a field of view of  $\sim 35' \times 35'$  and a scale of about  $\sim 0.25''/\text{pix}$ . The galaxy’s distance modulus is  $m - M = 26.43$  (Gieren et al. 2008). Accordingly, O and early-B supergiants with  $M_v \sim -6.5$  have an apparent magnitude  $V \lesssim 20$ , sufficient for low-resolution spectroscopy. Magnitude and colour ( $V - I$ )  $\lesssim 0.0$  were the main criteria for candidate selection. NGC 55 has a high galactic latitude ( $b = -75^\circ$ ) and the foreground reddening is low ( $E(B - V) = 0.013$ , Schlegel et al. 1998). Nonetheless, the internal reddening of the galaxy may not be negligible since NGC 55 is almost “edge-on”. In fact, the internal reddening affecting the Cepheids in NGC 55 has been estimated from a multiwavelength analysis in Gieren et al. (2008) to be  $E(B - V) = 0.13$ . Figure 1 shows the colour-magnitude diagram from which targets were selected, along with a plot identifying their positions in the galaxy.

The final list of candidates was built by careful examination of the images to reject objects with nearby companions (real or projected) and to avoid overlap with H II regions, a hard task

<sup>1</sup> <http://ezzelino.ifa.hawaii.edu/~bresolin/Araucaria/index.html>

**Table 1.** VLT-FORS2 observations of NGC 55.

Field	RA (J2000)	DEC (J2000)	Total $T_{exp}$ (s)	Date
A	00:15:55.0	-39:16:13.0	10800	2004-11-07
B	00:15:22.9	-39:13:54.6	13500	2004-11-10
C1	00:14:57.6	-39:12:28.5	10800	2004-11-06
C2	00:14:57.6	-39:12:28.5	10800	2004-11-06
D	00:14:25.5	-39:10:21.4	16200	2004-11-07/2004-11-10

given the inclination of the galaxy. We cannot eliminate the possibility that the targets are unresolved binaries, since at the distance of NGC 55 one arc-second corresponds to  $\sim 9.2$  pc. In fact, the occurrence of binarity in blue massive stars is quite high. According to Mason et al. (1998) in their study 72.2% of O-type stars in clusters are in binary systems, while the rate is 19.4% for field stars. In addition, the low spectral resolution of our data makes the detection of binaries from their spectra a difficult task.

We obtained spectra for  $\sim 200$  objects with FORS2 (FOcal Reducer and low dispersion Spectrograph, Appenzeller et al. (1998)) at the Very Large Telescope (VLT-UT2), in the Mask eXchange Unit (MXU) mode. The observations, performed in November 2004, are summarised in Table 1. The detector is a mosaic of two  $2k \times 4k$  MIT CCDs with a gap of  $4''$ . The total field of view is  $6'.8 \times 6'.8$ . Four pointings were necessary to cover the whole galaxy, as shown in Fig. 2. One mask per field was built with FIMS (FORS Instrumental Mask Simulator), except for the central pointing where the population of blue massive stars is expected to be dense and two masks were needed. The spectra were taken with the 600B grism which provided the highest resolving power for this study ( $\lambda/\Delta\lambda = 780$ ) in the wavelength range of interest (3100 – 6210Å). Each slit was carved with a width of 1 arc-second. The position of the target stars studied in this paper marked on the FORS2 V-band preimaging is shown in Figs. C.1 to C.5.

The spectra were reduced with the pipeline developed by Demarco et al. (2005) optimised for FORS2 data and upgraded for this work with the implementation of two new modules: van Dokkum (2001)'s algorithm for cosmic ray rejection, based on the laplacian edge detection; and a routine to normalise flat field images prior to performing the flat-field correction. The pipeline extracts all slits and works with them separately, taking into account the deformation of the slits on the CCD. The code then follows the standard steps for long slit spectrum reduction, using IRAF<sup>2</sup> tasks: bias, flat-field correction and background subtraction. The latter was the most challenging one, since in some instances we were unable to completely correct for nebular contamination. This was particularly problematic in the case of some of the Balmer lines which were filled with nebular emission (see below). The pipeline produces one-dimensional spectra with an optimised wavelength calibration. Finally, the individual exposures were combined (weighted by their count number) and rectified to the local continuum (normalised).

Sky subtraction was a laborious task due to nebular emission, which is particularly strong in the central regions of the galaxy. This contamination is more severe in young stars, which are still embedded in the dense regions where they were born. Interstellar absorption lines (Ca II  $\lambda 3933 - 3968$ ) can also contaminate the spectrum (Hartmann 1904). Moreover, given the high inclination of the galaxy, photons from a large number of H II regions

**Table 2.** Number of NGC 55 blue massive stars identified in this work, separated by field and spectral type.

Field	O-Type	B-Type	A-Type	WR-LBVc	Total
A	5	20	13	1	39
B	4	7	7	3	21
C	4	34	30	3	71
D	1	14	18	0	33
Total	14	75	68	7	164

(with different radial velocities) are integrated along the line of sight. One last problem in the sky subtraction is the low spectral resolution of the data. In spite of all our efforts, the spectra of several stars are strongly contaminated by the background. Nevertheless, in the vast majority of our targets the nebular lines do not compromise the spectral classification.

The reduced spectra have a signal-to-noise ratio (S/N) of  $\sim 75$  on average, sufficient for spectral classification. The spectra of the brightest objects with  $S/N \geq 100$  can be analysed quantitatively, which will be done in a future paper. A few objects are underexposed with S/N smaller than 50.

### 3. SPECTRAL CLASSIFICATION

The morphological analysis of stellar spectra is a crucial first step in studying the population of massive stars in a galaxy and provides clues about the stellar parameters of the stars. The main advantage of a classification system is that it preserves its independence from theoretical models or other external information (Walborn 1979).

The system developed by Morgan et al. (1943), together with subsequent refinements by Walborn & Fitzpatrick (1990) (hereafter WF) and Lennon et al. (1992), is the basis for the classification of Galactic stars. However, metallicity alters the strength of the metallic diagnostic lines and therefore the stellar classification criteria are dependent on the star's metallicity. In newly explored galaxies where the metallicity is not accurately known, we have to be cautious and use the appropriate standards, since the chemical composition of the studied stars may differ from all existing templates. In light of this, we also used as standards those of Fitzpatrick (1991) from the LMC and Lennon (1997) and Evans & Howarth (2003) from the Small Magellanic Cloud (SMC).

NGC 55 seems to have a metallicity similar to the LMC (Tüllmann et al. 2003; Davidge 2005). Following the idea of Fitzpatrick (1991), we have performed the spectral classification of our sample by visual comparison with templates from LMC stars. Even though the metallicities of both galaxies are similar, we have been careful with criteria involving both helium or hydrogen lines and metallic transitions. Criteria based only on metallic transitions, for instance Si III/Si IV, were preferred when available. The luminosity class was determined following WF for O-type stars and using the width of Balmer lines for B- and A-stars (Azzopardi 1987). We also took into account that

<sup>2</sup> IRAF is distributed by the National Optical Astronomy Observatory, which is operated by the Association of Universities for Research in Astronomy, Inc., under cooperative agreement with the National Science Foundation.

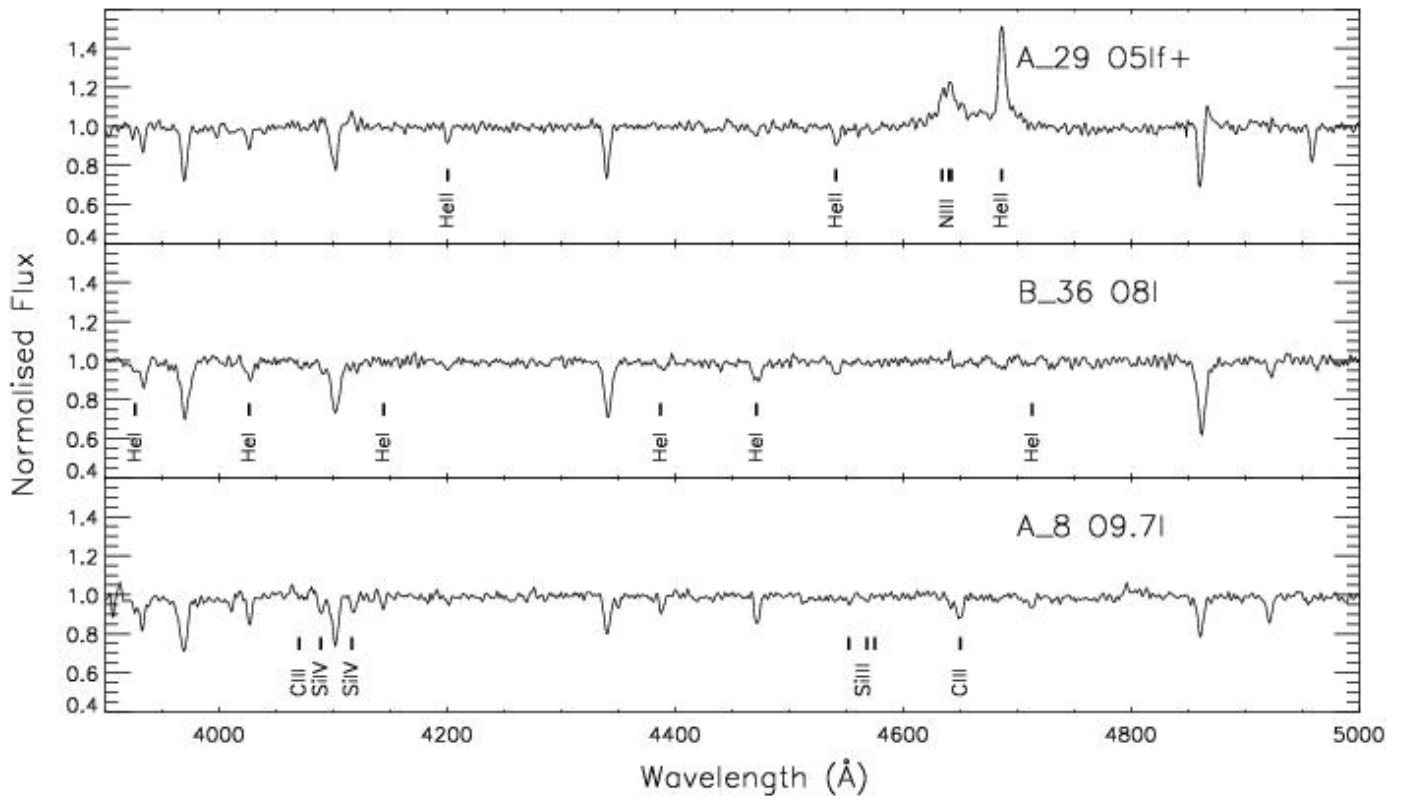


**Fig. 3.** O-type supergiants in NGC 55. The most relevant transitions for spectral classification are shown.

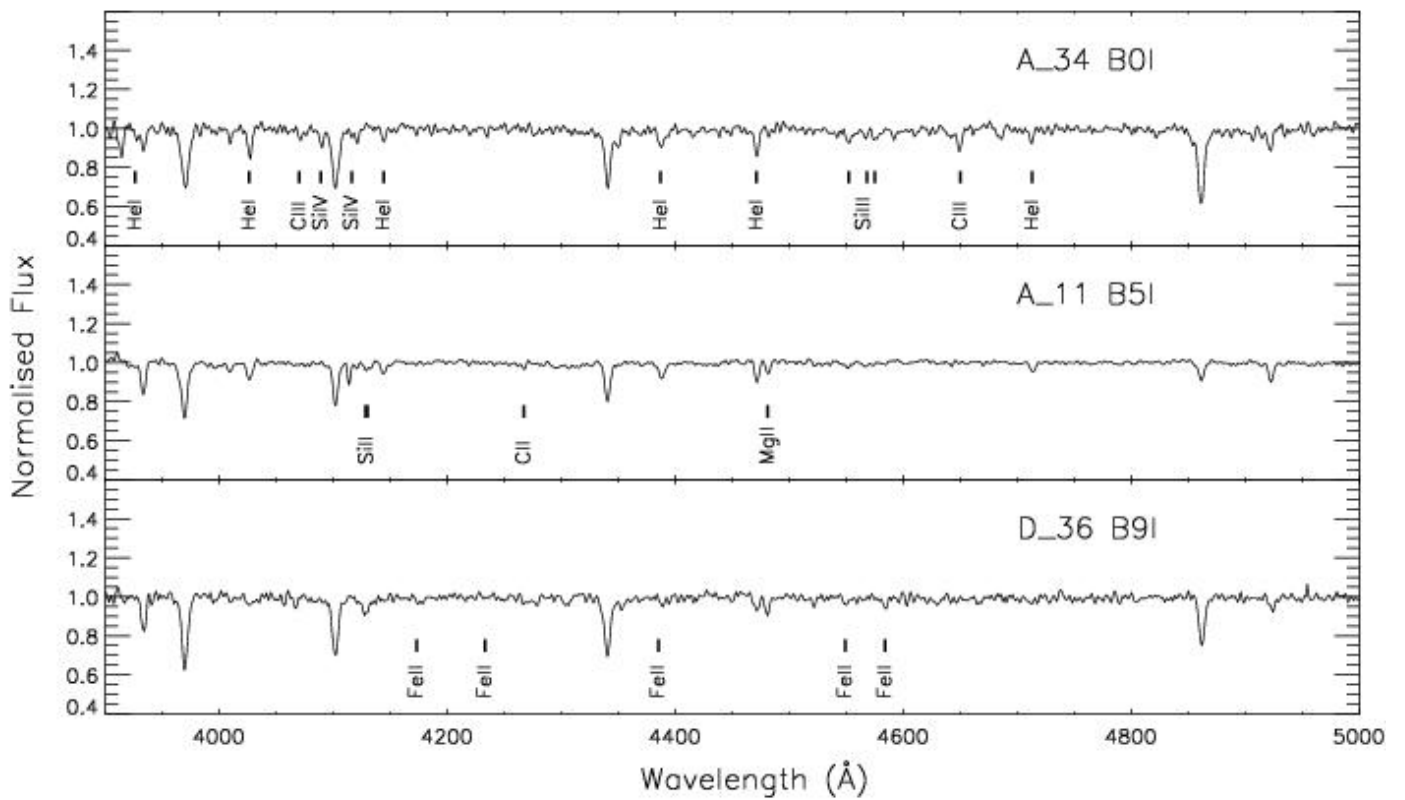


**Fig. 4.** Optical spectra of B-type supergiants in NGC 55.

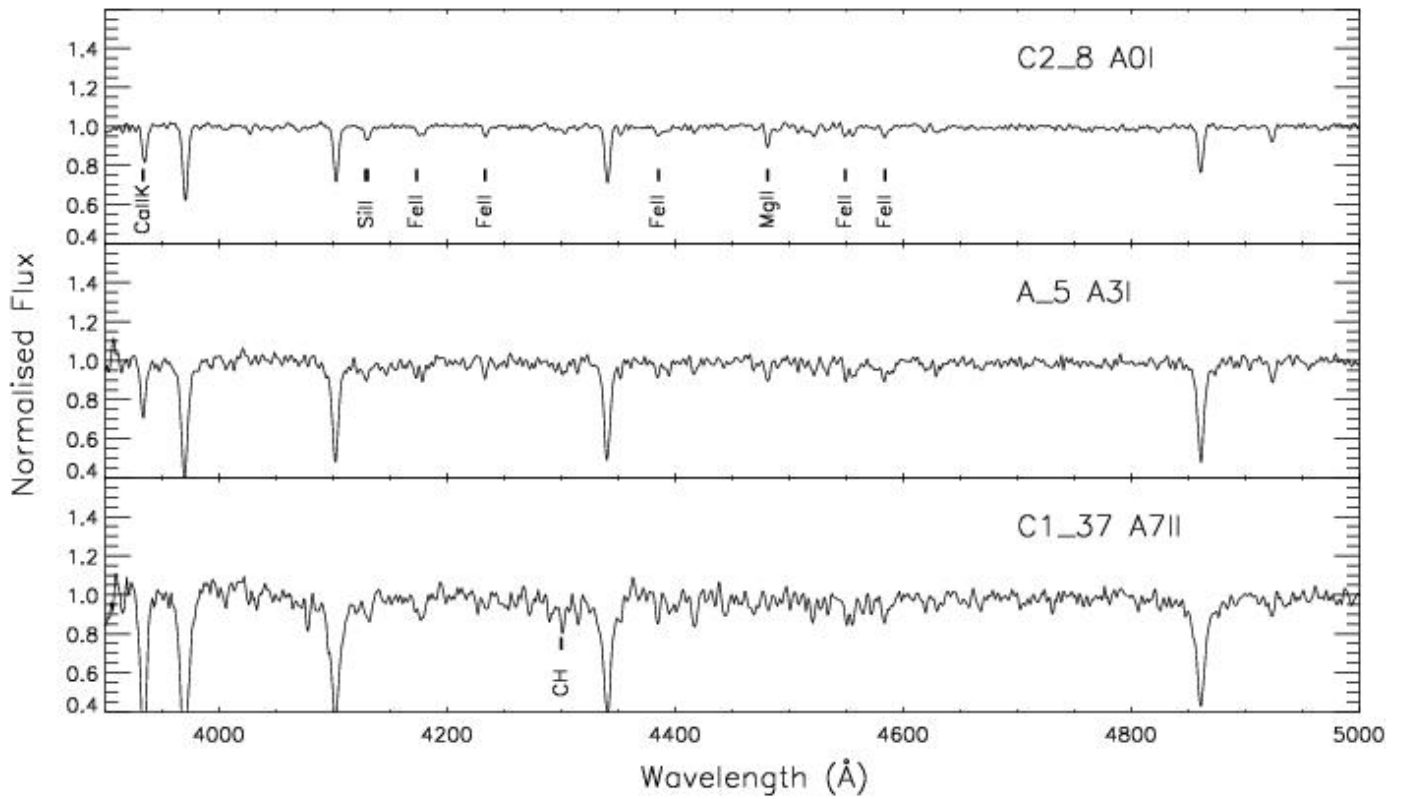


**Fig. 5.** Optical spectra of A-supergiants in NGC 55.

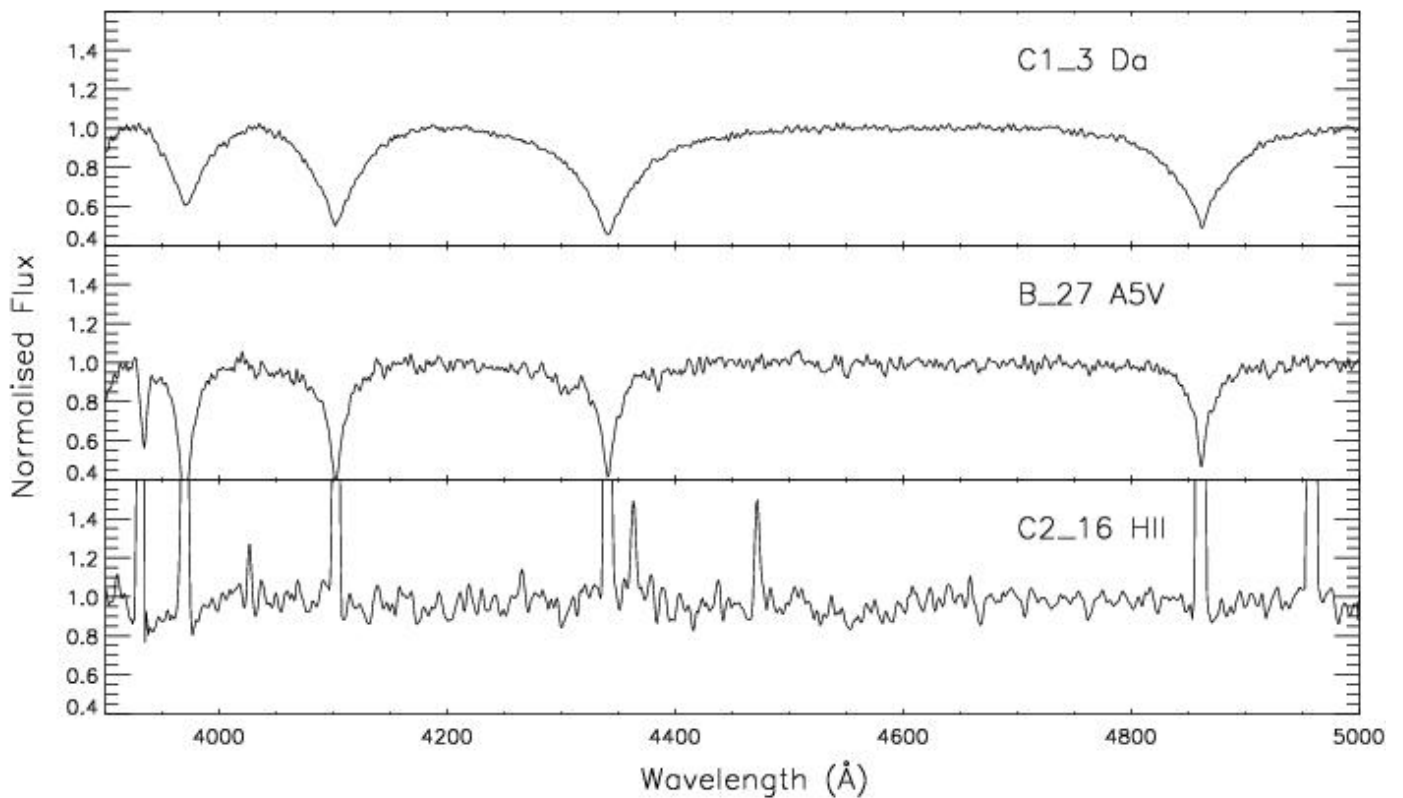


**Fig. 6.** Three exceptional cases: a white dwarf (top), an A5V detected in our sample probably belonging to the Milky Way halo (middle) and an example of spectra dominated by HII emission (bottom).

**Table 3.** A subset of blue massive stars showing a variety of spectral types (O-, B-, A-types plus WRs and LBV candidates, LBVc) observed in NGC 55.

ID	RA(J2000)	DEC(J2000)	V	V-I	Spectral Type	Rg	$v_r$	S/N	Metallicity	Comments
(1)	(2)	(3)	(4)	(5)	(6)	(7)	(8)	(9)	(10)	(11)
D_36	0:14:35.07	-39:11:20.04	19.189	-0.689	B9I	-278.26	78	70	LMC	
C2.8	0:14:43.87	-39:12:29.51	19.294	-0.652	A0I	-147.56	95	69	SMC	
C1_18	0:14:55.94	-39:11:21.84	19.316	-0.707	WN8	-37.95	124	30	-	neb.
C1_30	0:14:59.91	-39:12:11.88	18.921	-0.425	LBVc	95.62	158	28	-	
C1_37	0:15:02.50	-39:13:58.44	19.642	-0.588	A7II	153.43	146	55	-	
C1_51	0:15:14.70	-39:12:54.36	18.306	-0.098	Ope/WN9	319.21	187	57	-	neb.
B_12	0:15:16.68	-39:13:26.40	19.108	-0.666	O/WN	351.60	176	90	-	neb.
B_13	0:15:18.63	-39:13:12.72	18.543	-0.435	LBVc/WN11	379.26	274	103	-	
B_34	0:15:37.73	-39:13:49.08	19.533	-0.242	LBVc/WN11	667.26	216	35	-	
B_36	0:15:40.62	-39:13:40.07	19.782	-0.389	O8I	709.64	171	55	-	
A_5	0:15:40.83	-39:15:09.72	20.071	-0.495	A3I	722.43	260	58	-	
A_8	0:15:44.18	-39:14:58.20	19.792	-0.188	O9.7I	770.70	304	62	-	
A_11	0:15:45.17	-39:15:56.15	18.706	-0.245	B5I	793.59	209	130	LMC	
A_29	0:15:57.97	-39:15:33.84	19.575	-0.595	O5If+	980.35	210	62	-	neb.
A_34	0:16:01.17	-39:16:34.67	20.247	-0.875	B0I	1036.66	215	68	LMC	
A_42	0:16:09.69	-39:16:13.44	19.453	-0.189	LBVc	1160.17	175	75	-	

Note 1. The complete catalogue is gathered in Table A.1.

luminosity and spectral type are not independent. The resolution and quality of the spectra prevented us from doing a luminosity classification finer than I, II, III and V. Besides, the lack of H $\alpha$  spectra and the nebular contamination further impairs this distinction. Additional diagnostic metallic lines for luminosity class of B- and A-types exist (see for instance WF), but the variations are smaller given the low metallicity of NGC 55 and cannot be detected at the quality and resolution of the spectra.

We have provided detailed classifications for 204 spectra, out of which 164 stars seem to belong to NGC 55 and have spectral types earlier than F0. The rest of the objects include F- and G-supergiants (23 stars), H II regions (4 spectra) and a sample of B-, A-, F-, and G-dwarfs (13 stars) plus a white dwarf. The number of different types of blue massive stars found in NGC 55 is provided in Table 2. The complete catalogue is available in the appendices. Table A.1 lists the set of early-type stars (earlier than F0) found in NGC 55 (in Table 3 we show a fragment of the total database as an illustration, including some objects presented in following figures). The catalogue columns are: (1) star identification, consisting of field number followed by slit number; (2) right ascension (hh:mm:ss); (3) declination (dd:mm:ss); (4) V-magnitude; (5) V-I colour; (6) spectral type; (7) projected galactocentric distance (arc-seconds); (8) radial velocity (km s<sup>-1</sup>); (9) signal-to-noise ratio of the spectrum; (10) metallicity estimate; (11) comments. The corresponding digital spectral atlas is displayed in Figs. B.1 – B.21. F- and G-stars (classified using Jaschek & Jaschek 1990 and templates from Le Borgne et al. 2003) are compiled in Table A.2, for completeness. Finally, Table A.3 lists dwarf stars together with a Galactic white dwarf found in the sample.

The accuracy of the classification depends on several factors. It is essential to have spectra of sufficiently high S/N. Faint stars have been assigned only a very rough classification. A good subtraction of cosmic rays and a complete sky subtraction are key points. The latter was not always possible, leaving the Balmer lines (main luminosity class indicators) contaminated by nebular emission at their cores. However, the impact on the luminosity classification was negligible in most cases since we could use the Balmer line wings and the relevant metallic lines were not affected. We have marked the spectra with remaining nebular contamination in the Balmer lines or in the [O III] lines (about

46% of the sample) with comment ‘neb.’ in Tables 3, A.1, A.2 and A.3.

We have found a total of 14 O-type stars in our sample. Fig. 3 shows a subset of these objects. Most of the observed stars (75 of them) are B-type, some examples are presented in Fig. 4. We have classified 68 stars as A-type and some representative examples can be seen in Fig. 5. In these figures we have marked the most important lines used in the spectral classification, following the criteria cited above.

We have also studied a few spectra that display only strong emission lines and have poor S/N, which have been classified as H II regions (although the emission could actually be the result of the contribution from several H II regions). Figure 6 illustrates this case, and also includes an A-type star with low luminosity class and the white dwarf star. Stars with luminosity class V were discarded as members of NGC 55 and very likely belong to the Milky Way, since at the distance of NGC 55 a V-class star would be too faint to be observed. Although their radial velocities (see section 4) concur with the projected position on NGC 55, they are also consistent with the velocity of stars from the halo (Brown et al. 2006).

Twelve stars of the BA sample display the typical absorption lines of B- or A-type stars but broad emission in the wings of the Balmer lines. These might have a nebular origin, however the width of the wings suggests that they are dominated by stellar emission. A possible explanation for these features is a strong wind, but we might be witnessing a Be star, electron scattering or even an outburst stage of LBV where other distinctive features (like emission in Fe II lines) are masked by the low spectral resolution or are too weak (see Walborn & Fitzpatrick 2000, hereafter WF20). A\_42 (see Fig. 7) might be an extreme case, where the Balmer lines are completely in emission (see below). We have marked these objects with ‘*Str. winds?*’ in Table A.1.

### 3.1. WRs & LBV candidates

There are 7 NGC 55 blue stars in the sample that do not belong to the normal O, B or A spectral bins. Most of these objects are candidate WR or LBV stars. We referred to “The OB Zoo” of WF20 and references therein for their classification. The ni-

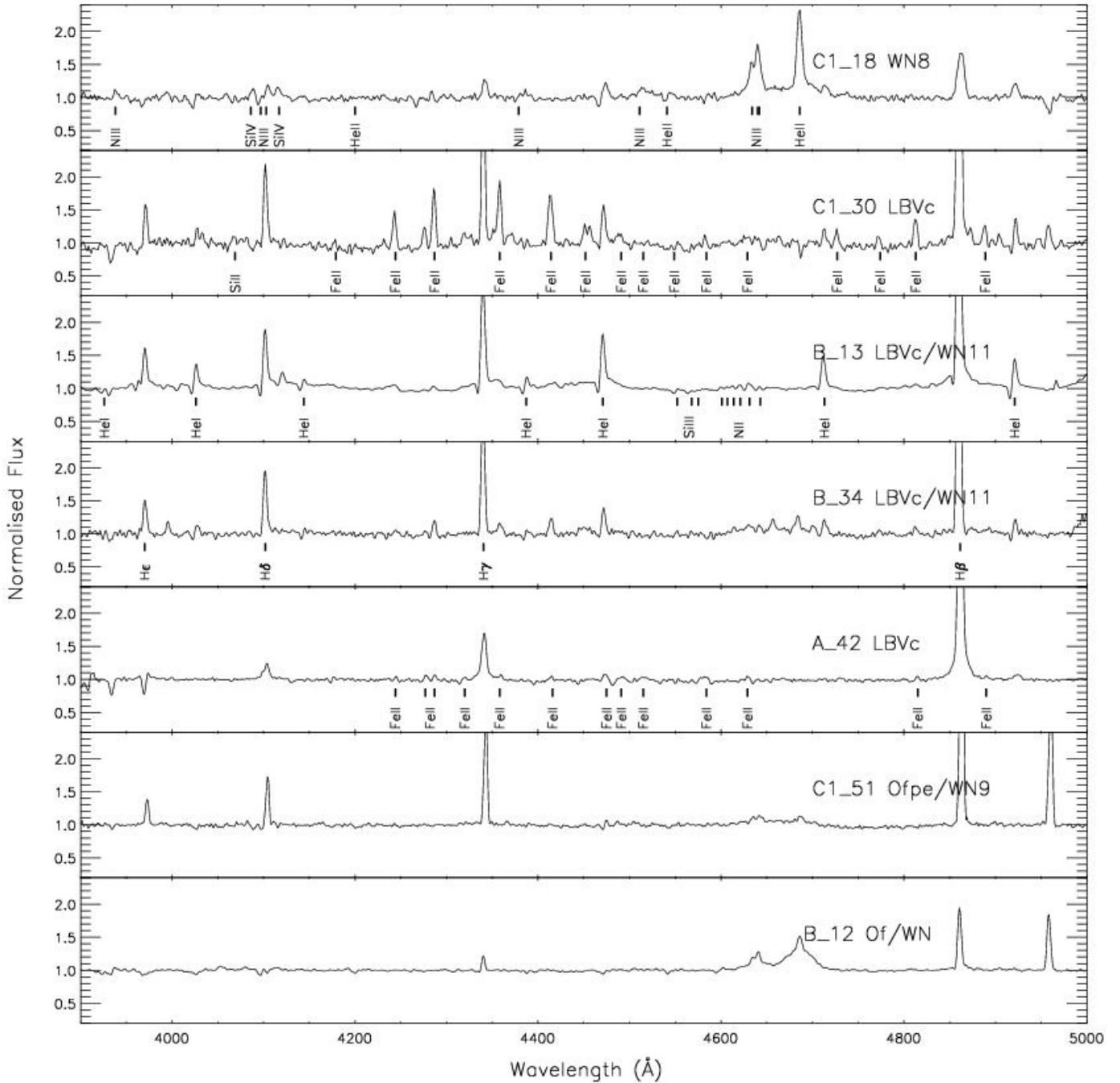


**Fig. 7.** “Exotic” stars found in our survey of NGC 55. See Sect. 3.1 for a discussion of the morphology of each object.

trogen WRs (WN) were also classified following the criteria of Smith et al. (1996) based on nitrogen and helium lines. The classification of LBVs is particularly difficult, since they undergo different stages during their evolution (Massey et al. 2007). We looked for similarities with the spectra of known LBVs or LBV candidates (these objects are marked as LBVc in Table 3 and A.1). The Fe II emission lines were a decisive factor in our identification of these objects.

Figure 7 presents the spectra of these peculiar emission line stars found in the sample. C1\_18 shows the typical features of a WN8 star, namely intense emission lines of He II $\lambda$ 4686 and N III $\lambda$ 4640. The templates from WF20 render C1\_30 as an iron star and an LBV candidate. Its spectrum is rich in emission lines

of hydrogen, helium and iron. Its overall morphology is very similar to that of the LBV “ $\eta$  Carinae”, considered by WF20 as “the mother of all iron stars”. B\_13 displays H and He I P Cygni profiles with strong emission of the hydrogen lines, resembling the morphology of “He3-519”, a possible LBV candidate or WN11 according to WF20. B\_34 falls into the same category, although the P Cygni profiles are weaker. These stars present several similar features with a star studied by Bresolin et al. (2002b) in NGC 300, classified as Ofpe/WN9. C1\_51 is classified as an Ofpe/WN9 due to its similarity with the objects presented in this group by WF20 and the digital atlas of Ofpe/WN9 of Bohannan & Walborn (1989). B\_12 has typical features of Of stars, however we have classified this star as Of/WN due to the broad

emission of He II  $\lambda 4686$ . The spectrum of A\_42 presents strong broad emission of Balmer lines that might be due to strong stellar winds. This is an A-star according to its Mg II, Si II and Ca II lines, but in this case the spectrum shows transitions of Fe II in emission. We conclude that this object is an LBV candidate. Finally, C1\_43 (not included in Fig. 7) shows features that might be interpreted as Fe II in emission, but its S/N is too poor to be conclusive.

#### 4. RADIAL VELOCITY

Radial velocities were determined from the Doppler wavelength shift of strong absorption lines (Balmer lines, He I, He II and metallic transitions of Mg II, Si III, depending on the spectral type). Alternative radial velocities were also evaluated from the emission lines of the surrounding nebula ([O III]  $\lambda 5007$ ) when available. Radial velocities were calculated in the heliocentric system. For the dates of the observations the correction was  $\sim -21 \text{ km s}^{-1}$ .

From the scatter in the individual determinations of the radial velocity of different lines we have obtained an average uncertainty of  $\sim 39 \text{ km s}^{-1}$  (note that in the case of nebular emission we have only used one line therefore the accuracy is smaller but enough to compare with the stellar data). Additional error sources apply, such as the wavelength calibration, but are of second order by comparison.

The resulting radial velocities are plotted in Fig. 8 as a function of the projected galactocentric distance, which is calculated with respect to the optical centre of NGC 55 ( $\alpha=00^h14^m53.60^s$ ,  $\delta=-39^d11^m47.9^s$  [J2000], Two Micron All Sky Survey team 2003). The results from nebular and stellar lines agree. We have also plotted the rotation curve derived from HI observations by Puche et al. (1991). The track was shifted  $1.5'$  to match the HI calculated rotation centre and the optical centre. Figure 8 shows how the stellar population traces the rotation of the galaxy, even in its outer parts. We obtain a systematic velocity (i. e. the radial velocity of NGC 55) of  $\sim 120 \text{ km s}^{-1}$ , very similar to the  $129 \text{ km s}^{-1}$  obtained by Koribalski et al. (2004). The fact that the young stellar population tracks the HI rotation curve has also been found in NGC 3109 by Evans et al. (2007).

The error bars of the results and the high inclination angle of NGC 55 prevent us from studying substructures in the galaxy, even though a few objects exhibit a radial velocity far from the normal behaviour of the stars. C2\_20 (B2I) has a very small radial velocity while B\_8 (O9If) presents a high radial velocity for its position in the galaxy. Figure 9 shows the spectra of these stars.

B\_8 is located in the middle of a cluster with H II regions seen in emission in the  $H\alpha$  image (see Fig. 10). Although this object presents absorption lines typical of an O-star, we are probably observing a group of stars. Its bright magnitude compared to other O-stars and the shape of the line profiles agree with this hypothesis. In addition, the spectrum is clearly affected by the nebular emission around the object.

The spectrum of C2\_20 exhibits no hint as to the reason for its small radial velocity. We have estimated a lower metallicity for C2\_20 (see section 5) and given its high galactic latitude, it might be a Galactic star of the halo with low metal content. However, this would be completely inconsistent with its classification as a supergiant since it would be brighter. Moreover, it is in the centre of NGC 55 and close to different clusters which show evidence of intense stellar activity. Therefore, we cannot exclude the possibilities that either a supernova explosion or binarity can be the cause of its peculiar radial velocity, although

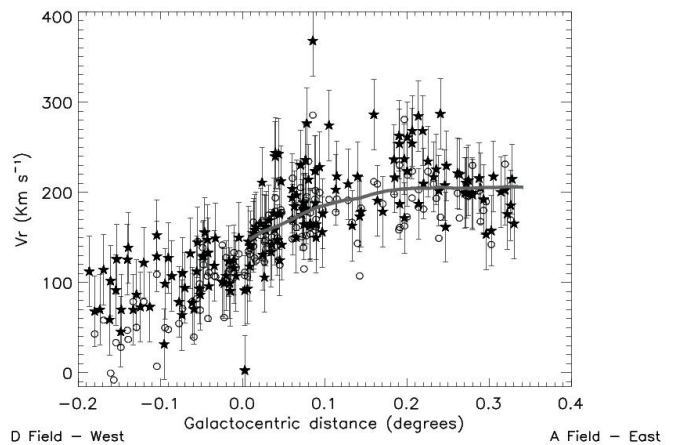


**Fig. 8.** Stellar radial velocities of NGC 55 blue stars as a function of the projected galactocentric distance (stars) and radial velocities measured from nebular emission (open circles). The galaxy's rotational curve derived by Puche et al. (1991) from HI regions (solid line) is included for comparison and there is good agreement with our results.

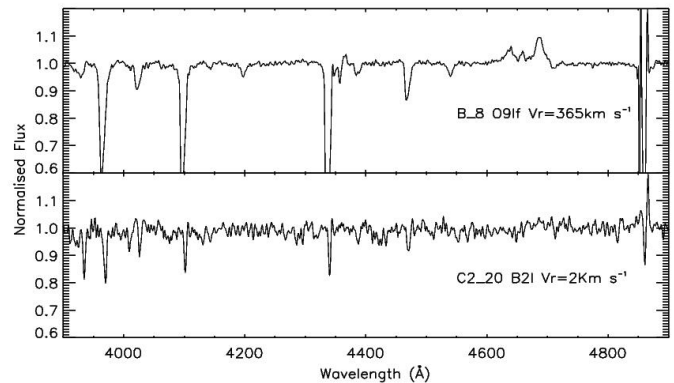


**Fig. 9.** Spectra of objects with anomalous radial velocity.

we must be cautious with this object due to the moderate S/N of its spectrum.

#### 5. METALLICITY: A ROUGH ESTIMATE

Studies based on different methods (Tüllmann et al. (2003), H II regions; Davidge (2005), stellar content) show that the chemical composition in the plane of NGC 55 is close to that of the LMC. We present here a qualitative estimate of the metal content of NGC 55. A subset of spectral lines of our stars are compared with objects of similar spectral type from the Milky Way (MW) (Lennon et al. 1992), LMC (Evans et al. 2006)<sup>3</sup> and SMC (Lennon 1997). This method has several caveats; the quality of our data, the use of different atlases for contrast and possible variations of the chemical composition of the comparison objects. While we have corrected for the diverse resolution of the standard spectra, we cannot account for other factors such as data reduction methods or slight differences in the spectral classification outcome. Nonetheless, the results will give us a flavour of the mean metallicity of the young stellar population and the

<sup>3</sup> These spectra were obtained in the VLT-FLAMES survey of massive stars in the Milky Way and the Magellanic Clouds (<http://star.pst.qub.ac.uk/~sjs/flames/>).

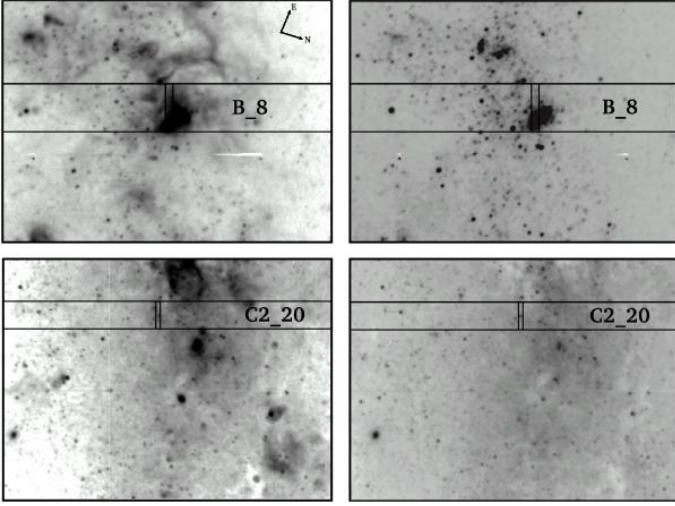


**Fig. 10.** V-band (right) and  $H\alpha$  (left) images taken with FORS2. The position of the slits used to observe B.8 (top) and C2.20 (bottom) are marked on the image. B.8 is near large H II structures, while C2.20 is located close the centre of NGC55.

possible presence of a chemical gradient. In a forthcoming paper we will perform a quantitative abundance analysis of a subset of blue massive stars in NGC 55.

The metallicity is estimated by comparing the strength of the lines of silicon ( $\text{Si IV } \lambda 4089$ ,  $\text{Si III } \lambda 4552 - 4568 - 4575$ ,  $\text{Si II } \lambda 4128 - 4130$ ) and magnesium ( $\text{Mg II } \lambda 4481$ ) found in NGC 55 stars to those observed in MW, SMC and LMC objects. Because the strength of these metallic lines depends on the stellar effective temperature and gravity, we have always used stars of the same spectral type and luminosity class (or as close as possible) for the comparison. Strong photospheric lines of carbon, oxygen and nitrogen exist in this wavelength range, but they can be contaminated by processed material from deeper layers due to mixing and evolution (Maeder & Meynet 2000; Hunter et al. 2008). Additional studies report a non-negligible underabundance of nitrogen in NGC 55 (possibly due to the galaxy being either young or deficient in lower mass stars relative to the LMC, Webster & Smith 1983; Aguero & Carranza 1985).

To illustrate the method two sample stars are compared to MW and Magellanic Clouds stars of similar spectral type in Fig. 11. The strength of silicon and magnesium transitions in the NGC 55 stars of the example resemble that of their LMC counterparts. The same analysis was performed on a set of supergiant stars between B0 and A0 (77 objects). We have distributed the stars into five metallicity bins (MW, MW-LMC, LMC, LMC-SMC, SMC) as we indicate in Tables 3 and A.1.

We find that the average metal content of the NGC 55 supergiants is similar to those of the LMC. At first glance the spatial distribution (see Fig. 12, left) does not show any systematic variation across the galaxy, in agreement with Webster & Smith (1983) who determined oxygen abundances from a small sample of bright H II regions in NGC 55. Nevertheless, if we plot the number of objects normalised by the total number of stars as a function of the projected galactocentric distance (see Fig. 12, right), some variation can be observed. At a projected galactocentric distance of 0.15 degrees and greater the population of stars with lower metallicity increases compared to the central population, where the majority of stars have LMC metallicity.

Once again, the high inclination angle of NGC 55 complicates our study. We cannot ensure that stars apparently close to

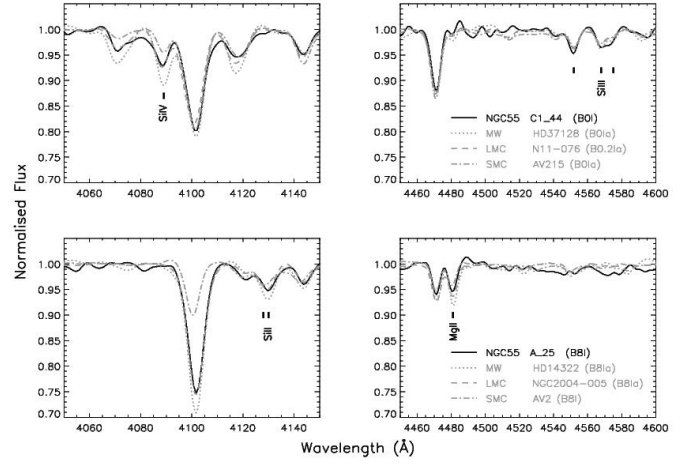


**Fig. 11.** Example of metallicity determination: the spectra of two NGC 55 stars, C1.44 (top) and A.25 (bottom), are compared to objects from the Milky Way, LMC and SMC with similar spectral types. In these cases the strength of the silicon and magnesium lines of the NGC 55 stars is similar to the LMC stars.

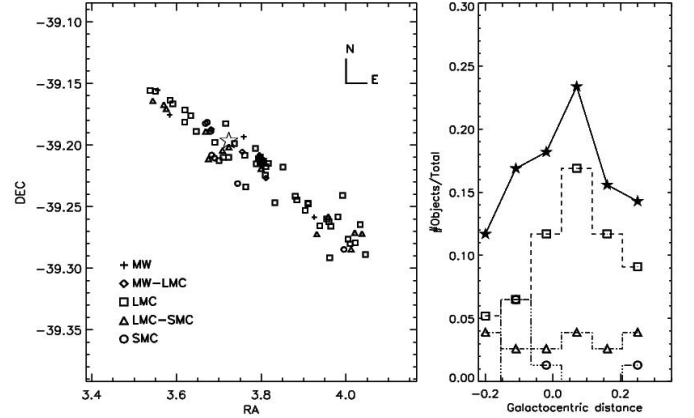


**Fig. 12.** Metallicity distribution of B0-A0 supergiants in NGC 55. Left: location of the sample stars in the galaxy, the different symbols indicate their metallicity as shown in the plot. The star shows the optical centre of the galaxy. The average metallicity is close to the LMC. Right: The number of objects per metallicity bin normalised by the total of stars considered, as a function of projected galactocentric radio (degrees). The histogram hints a variation across the projected disk of NGC 55. The solid line represents the stars in each bin over the total, thus giving an idea of how large is the sample in each position bin. We have not plotted the objects with MW and LMC-MW metallicity for clarity, since there are only four of them.

the centre are indeed in the disk of the galaxy and not in an outer layer but in the line of sight towards the centre. While the indirect evidence of a radial gradient found here cannot be considered significant until we perform a quantitative analysis, our exercise excludes a peculiar behaviour in our sample.

## 6. SUMMARY AND CONCLUSIONS

The long-term goal of our project is to obtain the physical parameters and abundances of blue massive stars in NGC 55. Results will be useful to study the evolution of massive stars

and its dependence with metallicity. The abundance measurements, representative of the clouds where the stars were born, are valuable input parameters to study the chemical evolution of the host galaxy. Another priority goal is to apply and test the Flux-Weighted Gravity-Luminosity Relation (Kudritzki et al. 2008) to the blue supergiant stars in NGC 55 to measure an independent spectroscopic distance to the galaxy. NGC 55 will be an excellent target for this given its abundant blue supergiant population.

As a first step, we have presented in this paper the first census of blue massive stars in NGC 55. The stars were identified from a qualitative analysis of their low-resolution optical spectra that yielded spectral classification for 204 objects with blue colours, out of which 164 have types earlier than F0.

We have also determined radial velocities from the observed spectra. In spite of the low wavelength accuracy and spectral resolution, we see a good agreement with the published rotation curve measured from HI (Puche et al. 1991). This study allowed us to detect one object with peculiar velocity that deserves a more detailed study.

A preliminary estimate of stellar metallicity, from the comparison of spectra with stars in the Milky Way, LMC and SMC, shows that the mean metal content of the stars is close to that of the LMC with some indication of a variation along the projected galactocentric distance. This requires confirmation by quantitative studies.

In a forthcoming paper, we plan to analyse the spectra of those blue massive stars with the highest S/N spectra with FASTWIND (Fast Analysis of STellar atmospheres with WINDs, Santolaya-Rey et al. 1997; Puls et al. 2005).

*Acknowledgements.* The authors would like to thank D. J. Lennon, M. A. Urbaneja and C. Evans for their help with the spectral classification and useful comments. D. J. Lennon is also acknowledged for his careful reading of the manuscript. We thank the FLAMES Survey of Massive Stars project (P.I. S. Smartt) for the LMC spectra. Finally, we are thankful to the referee for his/hers comments. WG and GP gratefully acknowledge financial support for this work from the Chilean Center for Astrophysics FONDAP 15010003. This project has been supported by Spanish grants AYA2004-08271-CO2-O1 and AYA2007-67456-CO2-O1.

## References

- Aguero, E. L. & Carranza, G. J. 1985, *Ap&SS*, 117, 271  
 Appenzeller, I., Fricke, K., Fürtig, W., et al. 1998, *The Messenger*, 94, 1  
 Azzopardi, M. 1987, *A&AS*, 69, 421  
 Bohannon, B. & Walborn, N. R. 1989, *PASP*, 101, 520  
 Bresolin, F., Gieren, W., Kudritzki, R.-P., Pietrzyński, G., & Przybilla, N. 2002a, *ApJ*, 567, 277  
 Bresolin, F., Kudritzki, R.-P., Mendez, R. H., & Przybilla, N. 2001, *ApJ*, 548, L159  
 Bresolin, F., Kudritzki, R.-P., Najarro, F., Gieren, W., & Pietrzyński, G. 2002b, *ApJ*, 577, L107  
 Bresolin, F., Pietrzyński, G., Urbaneja, M. A., et al. 2006, *ApJ*, 648, 1007  
 Bresolin, F., Urbaneja, M. A., Gieren, W., Pietrzyński, G., & Kudritzki, R.-P. 2007, *ApJ*, 671, 2028  
 Brown, W. R., Geller, M. J., Kenyon, S. J., & Kurtz, M. J. 2006, *ApJ*, 647, 303  
 Daflon, S. & Cunha, K. 2004, *ApJ*, 617, 1115  
 Davidge, T. J. 2005, *ApJ*, 622, 279  
 de Vaucouleurs, G. 1961, *ApJ*, 133, 405  
 Demarco, R., Rosati, P., Lidman, C., et al. 2005, *A&A*, 432, 381  
 Dufton, P. L., Smartt, S. J., Lee, J. K., et al. 2006, *A&A*, 457, 265  
 Evans, C. J., Bresolin, F., Urbaneja, M. A., et al. 2007, *ApJ*, 659, 1198  
 Evans, C. J. & Howarth, I. D. 2003, *MNRAS*, 345, 1223  
 Evans, C. J., Lennon, D. J., Smartt, S. J., & Trundle, C. 2006, *A&A*, 456, 623  
 Fitzpatrick, E. L. 1991, *PASP*, 103, 1123  
 Gieren, W., Pietrzyński, G., Bresolin, F., et al. 2005, *The Messenger*, 121, 23  
 Gieren, W., Pietrzyński, G., Soszyński, I., et al. 2008, *ApJ*, 672, 266  
 Hartmann, J. 1904, *ApJ*, 19, 268  
 Herrero, A., Corral, L. J., Villamariz, M. R., & Martín, E. L. 1999, *A&A*, 348, 542  
 Herrero, A., Puls, J., & Najarro, F. 2002, *A&A*, 396, 949  
 Hummel, E., Dettmar, R.-J., & Wielebinski, R. 1986, *A&A*, 166, 97  
 Hunter, I., Brott, I., Lennon, D. J., et al. 2008, *ApJ*, 676, L29  
 Hunter, I., Dufton, P. L., Smartt, S. J., et al. 2007, *A&A*, 466, 277  
 Jaschek, C. & Jaschek, M. 1990, *The Classification of Stars*. Cambridge Univ. Press, Cambridge.  
 Koribalski, B. S., Staveley-Smith, L., Kilborn, V. A., et al. 2004, *AJ*, 128, 16  
 Korn, A. J., Nieva, M. F., Daflon, S., & Cunha, K. 2005, *ApJ*, 633, 899  
 Kudritzki, R. P., Bresolin, F., & Przybilla, N. 2003, *ApJ*, 582, L83  
 Kudritzki, R.-P., Lennon, D. J., & Puls, J. 1995, in *Science with the VLT*, ed. J. R. Walsh & I. J. Danziger, 246–+  
 Kudritzki, R.-P. & Puls, J. 2000, *ARA&A*, 38, 613  
 Kudritzki, R. P., Puls, J., Lennon, D. J., et al. 1999, *A&A*, 350, 970  
 Kudritzki, R. P., Urbaneja, M. A., Bresolin, F., et al. 2008, *ApJ*, 999, 000  
 Le Borgne, J.-F., Bruzual, G., Pelló, R., et al. 2003, *A&A*, 402, 433  
 Lennon, D. J. 1997, *A&A*, 317, 871  
 Lennon, D. J., Dufton, P. L., & Crowley, C. 2003, *A&A*, 398, 455  
 Lennon, D. J., Dufton, P. L., & Fitzsimmons, A. 1992, *A&AS*, 94, 569  
 Lennon, D. J., Lee, J.-K., Dufton, P. L., & Ryans, R. S. I. 2005, *A&A*, 438, 265  
 Maeder, A. & Meynet, G. 2000, *ARA&A*, 38, 143  
 Mason, B. D., Gies, D. R., Hartkopf, W. I., et al. 1998, *AJ*, 115, 821  
 Massey, P. 2003, *ARA&A*, 41, 15  
 Massey, P., McNeill, R. T., Olsen, K. A. G., et al. 2007, *AJ*, 134, 2474  
 Mokiem, M. R., de Koter, A., Evans, C. J., et al. 2007, *A&A*, 465, 1003  
 Monteverde, M. I. & Herrero, A. 1998, *Ap&SS*, 263, 171  
 Monteverde, M. I., Herrero, A., & Lennon, D. J. 2000, *ApJ*, 545, 813  
 Morgan, W. W., Keenan, P. C., & Kellman, E. 1943, *An atlas of stellar spectra*. Chicago Univ. Press, Chicago  
 Muschelklo, B., Kudritzki, R. P., Appenzeller, I., et al. 1999, *A&A*, 352, L40  
 Pietrzyński, G., Gieren, W., Soszyński, I., et al. 2006, *AJ*, 132, 2556  
 Puche, D., Carignan, C., & Wainscoat, R. J. 1991, *AJ*, 101, 447  
 Puls, J., Urbaneja, M. A., Venero, R., et al. 2005, *A&A*, 435, 669  
 Rolleston, W. R. J., Smartt, S. J., Dufton, P. L., & Ryans, R. S. I. 2000, *A&A*, 363, 537  
 Rolleston, W. R. J., Venn, K., Tolstoy, E., & Dufton, P. L. 2003, *A&A*, 400, 21  
 Santolaya-Rey, A. E., Puls, J., & Herrero, A. 1997, *A&A*, 323, 488  
 Schlegel, D. J., Finkbeiner, D. P., & Davis, M. 1998, *ApJ*, 500, 525  
 Smartt, S. J., Venn, K. A., Dufton, P. L., et al. 2001, *A&A*, 367, 86  
 Smith, L. F., Shara, M. M., & Moffat, A. F. J. 1996, *MNRAS*, 281, 163  
 Trundle, C., Dufton, P. L., Hunter, I., et al. 2007, *A&A*, 471, 625  
 Trundle, C., Dufton, P. L., Lennon, D. J., Smartt, S. J., & Urbaneja, M. A. 2002, *A&A*, 395, 519  
 Trundle, C. & Lennon, D. J. 2005, *A&A*, 434, 677  
 Trundle, C., Lennon, D. J., Puls, J., & Dufton, P. L. 2004, *A&A*, 417, 217  
 Tüllmann, R., Rosa, M. R., Elwert, T., et al. 2003, *A&A*, 412, 69  
 Two Micron All Sky Survey team. 2003, *Extended objects*. Final release.  
 Urbaneja, M. A., Herrero, A., Bresolin, F., et al. 2005a, *ApJ*, 622, 862  
 Urbaneja, M. A., Herrero, A., Kudritzki, R.-P., et al. 2005b, *ApJ*, 635, 311  
 van Dokkum, P. G. 2001, *PASP*, 113, 1420  
 Venn, K. A., Lennon, D. J., Kaufer, A., et al. 2001, *ApJ*, 547, 765  
 Venn, K. A., McCarthy, J. K., Lennon, D. J., et al. 2000, *ApJ*, 541, 610  
 Venn, K. A., Tolstoy, E., Kaufer, A., et al. 2003, *AJ*, 126, 1326  
 Walborn, N. R. 1979, in *IAU Colloq. 47: Spectral Classification of the Future*, ed. M. F. McCarthy, A. G. D. Philip, & G. V. Coyne, 337  
 Walborn, N. R. & Fitzpatrick, E. L. 1990, *PASP*, 102, 379 (WF)  
 Walborn, N. R. & Fitzpatrick, E. L. 2000, *PASP*, 112, 50 (WF20)  
 Webster, B. L. & Smith, M. G. 1983, *MNRAS*, 204, 743

## Appendix A: Catalogue

**Table A.1.** Blue massive stars observed in NGC 55. We have also included spectra displaying only HII emissions. The columns list: (1) star identification, consisting on field number followed by slit number; (2) right ascension (hh:mm:ss); (3) declination (dd:mm:ss); (4) V-magnitude; (5) V-I colour; (6) spectral type; (7) projected galactocentric distance (arc-seconds); (8) radial velocity (km s<sup>-1</sup>); (9) signal-to-noise ratio of the spectrum; (10) metallicity estimate; (11) comments.

ID	RA(J2000)	DEC(J2000)	V	V-I	Spectral Type	Rg	$v_r$	S/N	Metallicity	Comments
(1)	(2)	(3)	(4)	(5)	(6)	(7)	(8)	(9)	(10)	(11)
D_1	0:14:08.97	-39:09:20.88	20.212	-0.557	B9I	-671.79	112	43	LMC	
D_3	0:14:10.51	-39:09:50.76	18.581	-0.407	A0I	-647.94	67	117	LMC-SMC	Str. winds?
D_4	0:14:12.11	-39:09:23.41	19.724	-0.524	B9I	-625.02	69	60	LMC	
D_5	0:14:13.22	-39:09:19.79	19.963	-0.813	B3I	-608.56	113	44	MW	
D_6	0:14:15.09	-39:08:50.28	19.367	-0.404	A3II	-582.18	58	62	-	
D_7	0:14:15.24	-39:09:29.87	19.928	-0.375	A0I-II	-578.13	101	52	-	
D_9	0:14:16.74	-39:10:02.28	19.355	-0.563	B5I	-554.71	91	93	LMC-SMC	
D_12	0:14:16.84	-39:11:25.08	20.096	-0.466	A0I-II	-551.43	125	45	-	
D_11	0:14:18.14	-39:10:14.16	18.447	-0.595	B3I	-533.37	45	199	LMC-SMC	neb. Str. winds?
D_10	0:14:18.35	-39:09:37.08	20.026	-0.516	A2I	-531.61	69	44	-	neb.
D_14	0:14:20.02	-39:10:32.15	20.582	-0.728	B2.5I	-504.73	125	30	MW	neb.
D_13	0:14:20.39	-39:09:49.32	20.375	-0.787	B1I	-500.77	138	42	LMC	
D_15	0:14:21.82	-39:10:00.11	20.258	-0.359	A0I	-479.02	69	43	LMC	
D_16	0:14:22.80	-39:09:51.83	20.199	-0.868	B0.5II	-464.75	86	30	-	neb.
D_25	0:14:23.76	-39:11:45.95	20.162	-0.449	A5II	-447.53	72	38	-	
D_23	0:14:24.92	-39:10:00.11	19.330	-0.743	B2.5II	-432.89	121	58	-	
D_24	0:14:26.77	-39:09:43.20	20.593	-0.455	A3II	-406.43	72	16	-	neb.
D_28	0:14:28.63	-39:10:53.04	19.613	-0.784	B0.5I	-375.37	128	32	LMC	neb.
D_27	0:14:28.73	-39:10:17.76	19.191	-0.642	B2I	-375.34	152	76	LMC	
D_29	0:14:31.14	-39:10:16.32	18.972	-0.456	A3I	-339.62	98	84	-	
D_26	0:14:31.87	-39:07:57.73	17.669	-0.073	A5I	-343.49	22	174	-	
D_31	0:14:32.04	-39:10:34.68	19.951	-0.767	B2I	-325.28	127	29	LMC	
D_32	0:14:33.14	-39:10:21.36	19.733	-0.567	A2I	-309.70	107	40	-	
D_36	0:14:35.07	-39:11:20.04	19.189	-0.689	B9I	-278.26	78	70	LMC	
D_38	0:14:36.07	-39:11:34.45	19.184	-0.427	A7II	-263.07	110	49	-	
D_35	0:14:36.29	-39:09:59.40	18.506	-0.462	A3I	-264.98	63	94	-	neb.
D_37	0:14:36.88	-39:10:45.12	19.926	-0.392	A3II	-252.70	93	25	-	
D_39	0:14:38.46	-39:10:48.36	18.313	-0.453	A2I	-228.94	132	100	-	
D_40	0:14:39.02	-39:10:57.00	19.903	0.165	A3III	-220.17	77	27	-	
C2_2	0:14:39.42	-39:12:19.81	19.704	-0.463	A2II	-213.33	70	55	-	
D_42	0:14:40.33	-39:10:57.35	18.700	-0.801	B1.5I	-200.63	112	53	SMC	neb.
C1_1	0:14:40.51	-39:11:20.04	18.893	-0.732	A0I	-196.85	144	100	LMC-SMC	
D_43	0:14:41.08	-39:11:12.84	19.454	-0.017	O9I	-188.62	92	27	-	
C2_1	0:14:41.38	-39:10:53.76	19.249	-0.641	A0I	-185.32	86	68	SMC	
C1_5	0:14:42.10	-39:12:40.32	19.249	-0.794	B2.5I	-174.61	128	82	LMC-SMC	
D_45	0:14:42.25	-39:11:15.36	19.737	-0.493	A2I	-171.10	129	45	-	neb.
D_46	0:14:42.58	-39:11:27.61	19.141	0.006	Late_AII	-165.57	155	19	-	
C1_4	0:14:43.39	-39:11:20.04	18.863	-0.606	B1.5I	-153.82	147	71	SMC	
C2_5	0:14:43.57	-39:11:14.29	19.215	-0.832	B3I	-151.41	132	55	MW-LMC	
C2_8	0:14:43.87	-39:12:29.51	19.294	-0.652	A0I	-147.56	95	69	SMC	
C1_9	0:14:45.54	-39:12:38.17	18.939	-0.817	B1I	-123.77	118	86	SMC	
C1_8	0:14:45.70	-39:11:52.08	18.920	-0.791	B8I	-118.58	149	72	LMC	
C1_10	0:14:47.70	-39:11:57.48	17.982	-0.495	A2I	-88.64	100	138	-	
C2_14	0:14:48.05	-39:12:45.72	19.044	-0.944	B8I	88.67	130	112	LMC	
C2_11	0:14:48.33	-39:11:20.75	18.545	-1.800	O8I	-80.41	98	67	-	neb.
C2_12	0:14:48.84	-39:11:24.00	19.006	-0.064	A2III	-72.60	107	73	-	neb.
C1_11	0:14:49.80	-39:11:07.43	19.444	-0.761	A3I	-60.99	123	46	-	neb.
C2_15	0:14:50.00	-39:12:16.19	19.424	-0.542	A0I	-56.07	98	83	LMC-SMC	
C2_13	0:14:50.21	-39:11:17.16	18.822	-0.710	A2I	-53.43	90	89	-	
C1_15	0:14:50.50	-39:12:36.35	19.642	-0.765	B8I	53.31	158	69	LMC	neb.
C1_16	0:14:51.16	-39:12:47.88	18.917	-0.588	A5I	48.87	154	98	-	
C1_13	0:14:51.86	-39:10:57.35	18.948	-0.706	B1I	-37.92	115	60	LMC	neb.
C2_16	0:14:52.28	-39:11:26.52	18.419	-0.451	HII	-22.95	109	24	-	
C2_18	0:14:52.32	-39:12:05.76	19.453	-0.591	B2.5II	21.52	92	42	-	
C1_14	0:14:52.59	-39:11:04.21	18.503	-0.662	A5I	-28.25	107	125	-	
C1_17	0:14:52.67	-39:12:38.88	18.830	-0.416	A3I	31.14	117	107	-	
C2_17	0:14:52.76	-39:11:29.04	18.748	-0.902	B0.5I	-16.32	149	51	-	

C2_19	0:14:53.13	-39:12:00.00	19.070	-0.371	A3I	9.71	91	46	-	neb.
C2_21	0:14:53.46	-39:12:35.64	19.719	-0.662	B2I	26.30	145	30	LMC	neb.
C2_20	0:14:53.58	-39:12:06.11	18.745	-0.262	B2I	10.01	2	65	LMC-SMC	neb.
C2_22	0:14:55.19	-39:12:30.96	18.764	-0.418	A2I	33.71	140	48	-	neb. Str. winds?
C1_18	0:14:55.94	-39:11:21.84	19.316	-0.707	WN8	-37.95	124	30	-	neb.
C2_29	0:14:56.75	-39:11:56.40	18.335	-0.638	B8I	47.50	150	63	LMC	neb.
C1_27	0:14:57.48	-39:12:00.00	19.274	-0.093	A2I	58.56	161	24	-	neb.
C2_33	0:14:58.50	-39:12:38.88	19.645	-2.167	O5III	79.00	165	42	-	neb.
C1_32	0:14:58.59	-39:13:52.68	17.122	-0.563	B9I	102.93	161	241	SMC	Str. winds?
C2_32	0:14:58.69	-39:12:15.12	18.164	-0.940	HII	77.93	139	28	-	neb.
C2_34	0:14:58.73	-39:12:54.00	19.062	-0.679	A3III	85.57	210	41	-	neb.
C2_35	0:14:59.68	-39:12:42.84	18.193	-1.404	Early_OI	96.38	105	34	-	neb.
C2_40	0:14:59.90	-39:14:12.11	19.428	-0.758	A7II	125.41	133	39	-	neb.
C1_30	0:14:59.91	-39:12:11.88	18.921	-0.425	LBV	95.62	158	28	-	LBV-Candidate
C1_31	0:15:00.01	-39:12:41.39	18.523	-0.716	Early_OI	100.92	157	40	-	neb.
C2_37	0:15:01.19	-39:12:20.16	18.909	-0.752	A0I	115.33	168	51	MW-LMC	neb.
C2_36	0:15:02.11	-39:11:35.87	19.325	-0.787	B8I	127.83	142	28	MW	neb.
C1_36	0:15:02.36	-39:13:31.44	19.287	-1.950	HII	144.48	162	22	-	neb.
C1_37	0:15:02.50	-39:13:58.44	19.642	-0.588	A7II	153.43	146	55	-	neb.
C1_34	0:15:02.58	-39:12:30.60	18.962	-0.789	B8I	137.00	176	69	LMC	neb.
C2_41	0:15:02.82	-39:12:58.68	18.475	-0.739	B0.5III	144.22	243	82	-	neb.
C1_35	0:15:02.85	-39:12:49.67	19.336	-0.534	B5III	143.30	239	52	-	neb.
C2_39	0:15:02.98	-39:12:05.04	18.180	-0.719	A2I	140.99	158	112	-	neb.
C1_38	0:15:03.16	-39:14:02.03	19.603	-0.849	B0I	163.24	175	38	LMC	neb.
C2_38	0:15:03.96	-39:11:04.92	18.586	-0.397	A3II	157.46	242	97	-	neb.
C2_44	0:15:04.10	-39:13:44.40	19.902	-0.725	A2I	171.66	141	51	-	neb.
C2_42	0:15:04.15	-39:12:51.84	20.382	-0.320	A7II	162.62	124	30	-	neb.
C2_43	0:15:04.19	-39:13:22.80	19.985	-0.687	B9II	168.27	212	30	-	neb.
C1_39	0:15:04.72	-39:13:52.32	18.514	-1.517	HII	182.16	132	22	-	neb.
B_3	0:15:07.65	-39:13:21.71	20.556	-0.165	A2II	218.02	193	33	-	neb.
C1_41	0:15:07.65	-39:13:21.71	20.556	-0.165	A3II	218.02	203	41	-	neb.
C2_45	0:15:08.05	-39:12:45.01	20.229	-0.299	A3II	219.39	169	26	-	neb.
C1_40	0:15:08.71	-39:12:09.73	20.010	-0.627	B1.5I	227.06	184	59	LMC	neb.
C1_42	0:15:09.00	-39:13:04.79	17.754	-0.277	A2I	235.59	149	137	-	Str. winds?
C2_46	0:15:09.18	-39:12:55.44	18.941	-0.672	B1I	237.18	196	75	LMC	neb.
C2_47	0:15:10.45	-39:12:39.97	19.459	-0.508	B9I	254.68	230	43	LMC	neb.
C1_43	0:15:10.86	-39:12:28.80	19.055	-0.069	A0I	260.17	175	57	LMC-SMC	Str. winds?
C1_46	0:15:11.18	-39:13:18.12	19.887	-0.439	B2III	269.43	164	27	-	neb.
C2_48	0:15:11.24	-39:12:38.17	19.371	-0.456	B5I	266.36	188	58	LMC	neb.
C1_44	0:15:11.29	-39:12:34.55	19.037	-0.740	B0I	266.90	181	79	LMC	neb.
C1_45	0:15:11.31	-39:12:50.40	19.607	-0.180	B1I	268.32	179	38	LMC	neb.
C2_49	0:15:11.82	-39:12:43.92	20.154	-0.570	B1I	275.40	235	33	LMC	neb.
C1_47	0:15:11.92	-39:13:08.76	18.023	-0.291	A0I	279.16	182	134	LMC-SMC	Str. winds?
C2_50	0:15:12.18	-39:12:52.56	20.159	-0.433	B1I	281.50	276	34	LMC	neb.
C2_51	0:15:12.68	-39:12:56.51	19.719	-0.764	B9I	289.24	213	61	MW-LMC	neb.
C1_48	0:15:13.11	-39:12:47.16	19.519	-0.715	B0.5I	294.93	164	30	LMC	neb.
C1_49	0:15:13.14	-39:13:01.20	19.127	-0.262	A5I	296.62	165	92	-	neb.
B_7	0:15:13.31	-39:12:43.56	17.595	-0.556	A0I	297.60	162	125	LMC-SMC	neb. Str. winds?
B_8	0:15:13.98	-39:12:48.25	15.874	-1.606	O9If	308.04	367	185	-	Cluster. neb.
C2_54	0:15:14.34	-39:13:27.84	19.435	-0.497	B9I	317.20	223	51	LMC	neb.
C1_53	0:15:14.64	-39:13:36.12	19.816	-0.485	B2.5I	322.60	164	45	MW-LMC	neb.
B_9	0:15:14.66	-39:13:03.72	19.416	-0.524	B5I	319.34	223	57	LMC	neb.
C1_51	0:15:14.70	-39:12:54.36	18.306	-0.098	Ofpe/WN9	319.21	187	57	-	neb.
C1_52	0:15:14.79	-39:13:10.92	18.542	-0.147	A2I	322.06	149	107	-	neb. Str. winds?
C2_55	0:15:15.95	-39:12:54.36	19.185	-0.277	B5I	337.85	228	39	LMC	neb.
B_12	0:15:16.68	-39:13:26.40	19.108	-0.666	Of/WN	351.60	176	90	-	neb.
B_11	0:15:16.74	-39:12:46.08	19.001	0.206	B1I	349.09	155	61	-	neb.
B_13	0:15:18.63	-39:13:12.72	18.543	-0.435	LBV/WN11	379.26	274	103	-	LBV-Candidate
B_22	0:15:19.73	-39:14:48.12	18.274	-0.268	B2.5I	408.46	202	143	LMC	Str. winds?
B_15	0:15:20.89	-39:13:17.76	20.308	-0.161	A3I	413.34	217	29	-	neb.
B_23	0:15:24.24	-39:13:04.79	19.531	-0.586	B2I	462.36	209	77	LMC	neb.
B_24	0:15:25.44	-39:13:03.00	20.318	-0.300	A5II	480.06	162	43	-	neb.
B_26	0:15:26.91	-39:13:28.92	20.116	-0.891	O9I	504.13	217	52	-	neb.
B_28	0:15:27.41	-39:14:36.60	19.591	-0.079	A0III	519.32	178	56	-	neb.

B_25	0:15:27.78	-39:12:25.56	18.712	-0.261	A0III	513.24	173	74	-	
B_30	0:15:31.27	-39:14:30.12	19.591	-0.012	B9I	575.47	291	74	LMC	neb. Str. winds?
B_31	0:15:32.22	-39:14:40.20	19.429	-0.478	B2.5I	590.90	190	95	LMC	
B_33	0:15:33.53	-39:15:10.44	19.125	-0.467	O5If	614.56	178	94	-	neb.
B_35	0:15:36.86	-39:15:10.79	20.291	-0.513	B1.5I	663.87	236	30	LMC	neb.
B_34	0:15:37.73	-39:13:49.08	19.533	-0.242	LBV/WN11	667.26	216	35	-	LBV-Candidate
B_37	0:15:38.38	-39:15:29.88	19.651	-0.201	A2I	689.16	186	53	-	neb.
A_1	0:15:38.52	-39:14:49.21	19.099	-0.777	B1I	685.46	262	110	LMC	neb.
A_2	0:15:38.64	-39:14:52.43	19.227	-0.632	B1.5I	687.62	253	77	LMC	neb.
A_4	0:15:39.99	-39:15:00.71	19.604	-0.167	A5I	708.86	236	71	-	neb.
B_36	0:15:40.62	-39:13:40.07	19.782	-0.389	O8I	709.64	171	55	-	
A_5	0:15:40.83	-39:15:09.72	20.071	-0.495	A3I	722.43	260	58	-	
A_3	0:15:41.35	-39:13:48.73	19.623	-0.184	A2I	721.24	223	86	-	neb.
A_7	0:15:41.99	-39:15:30.95	19.901	-0.650	B2I	742.73	254	73	MW	
A_6	0:15:42.47	-39:14:46.32	19.039	-0.199	A3I	743.83	268	86	-	
A_10	0:15:43.43	-39:16:20.28	18.836	-0.329	A0I	772.06	187	134	LMC-SMC	
A_8	0:15:44.18	-39:14:58.20	19.792	-0.188	O9.7I	770.70	304	62	-	
A_11	0:15:45.17	-39:15:56.15	18.706	-0.245	B5I	793.59	209	130	LMC	
A_9	0:15:45.56	-39:14:45.59	18.824	-0.175	A5I	789.71	268	84	-	
A_12	0:15:46.52	-39:15:48.96	18.594	-0.722	O5If	812.49	234	129	-	neb.
A_13	0:15:48.53	-39:15:14.04	20.310	-0.195	A5II	837.32	216	44	-	
A_14	0:15:49.14	-39:15:35.64	19.139	-0.279	B9I	849.33	225	115	LMC	neb.
A_15	0:15:49.93	-39:15:28.80	18.794	-0.475	B3I	860.21	201	154	LMC-SMC	neb. Str. winds?
A_16	0:15:50.25	-39:15:43.92	19.590	-0.518	B0.5I	867.08	286	121	LMC	neb.
A_25	0:15:50.78	-39:17:29.40	19.687	-0.504	B8I	893.29	229	86	LMC	
A_18	0:15:51.38	-39:16:20.28	19.555	-0.019	A7I	889.45	161	100	-	neb.
A_17	0:15:51.42	-39:15:57.60	20.336	-0.321	B1I	886.44	207	79	LMC	
A_26	0:15:55.45	-39:15:30.60	19.236	-0.262	B2.5I	942.47	220	96	LMC	
A_28	0:15:55.62	-39:16:11.27	20.047	-0.336	A2I	950.75	219	62	-	
A_30	0:15:57.58	-39:16:14.51	19.468	-0.795	O9I	980.26	199	44	-	neb.
A_29	0:15:57.97	-39:15:33.84	19.575	-0.595	O5If+	980.35	210	62	-	neb.
A_27	0:15:58.03	-39:14:27.60	19.928	-0.477	B2I	973.83	199	66	LMC	
A_31	0:15:58.22	-39:16:14.16	20.288	-0.592	O9I	989.71	213	46	-	neb.
A_33	0:15:58.83	-39:17:05.29	19.996	-0.429	A0I	1007.21	199	75	SMC	
A_32	0:15:59.49	-39:16:08.40	17.813	-0.335	A7I	1007.73	197	141	-	neb.
A_34	0:16:01.17	-39:16:34.67	20.247	-0.875	B0I	1036.66	215	68	LMC	
A_35	0:16:01.49	-39:16:42.96	19.744	-0.490	B3III	1042.77	204	80	-	
A_36	0:16:02.33	-39:16:48.72	20.758	-0.418	B2I	1056.24	191	39	LMC	neb.
A_37	0:16:02.90	-39:17:04.91	20.024	-0.603	B0.5I	1067.34	153	71	LMC-SMC	neb.
A_38	0:16:04.95	-39:16:15.96	18.706	-0.197	A0I	1089.96	157	146	LMC-SMC	
A_39	0:16:05.30	-39:16:45.84	20.451	-0.021	B5I	1099.75	217	51	LMC	
A_40	0:16:08.02	-39:15:52.20	19.938	-0.484	B5I	1132.32	200	67	LMC	
A_41	0:16:09.00	-39:16:18.84	20.114	-0.445	B1I	1150.65	202	52	LMC-SMC	neb.
A_42	0:16:09.69	-39:16:13.44	19.453	-0.189	LBV	1160.17	175	75	-	LBV-Candidate
A_43	0:16:10.57	-39:16:27.48	19.358	-0.215	A2I	1175.18	185	94	-	neb.
A_44	0:16:10.91	-39:16:33.25	20.103	-0.443	B3II	1181.10	214	49	-	neb.
A_45	0:16:10.98	-39:17:19.68	20.710	-0.726	B0I	1189.70	165	44	LMC	

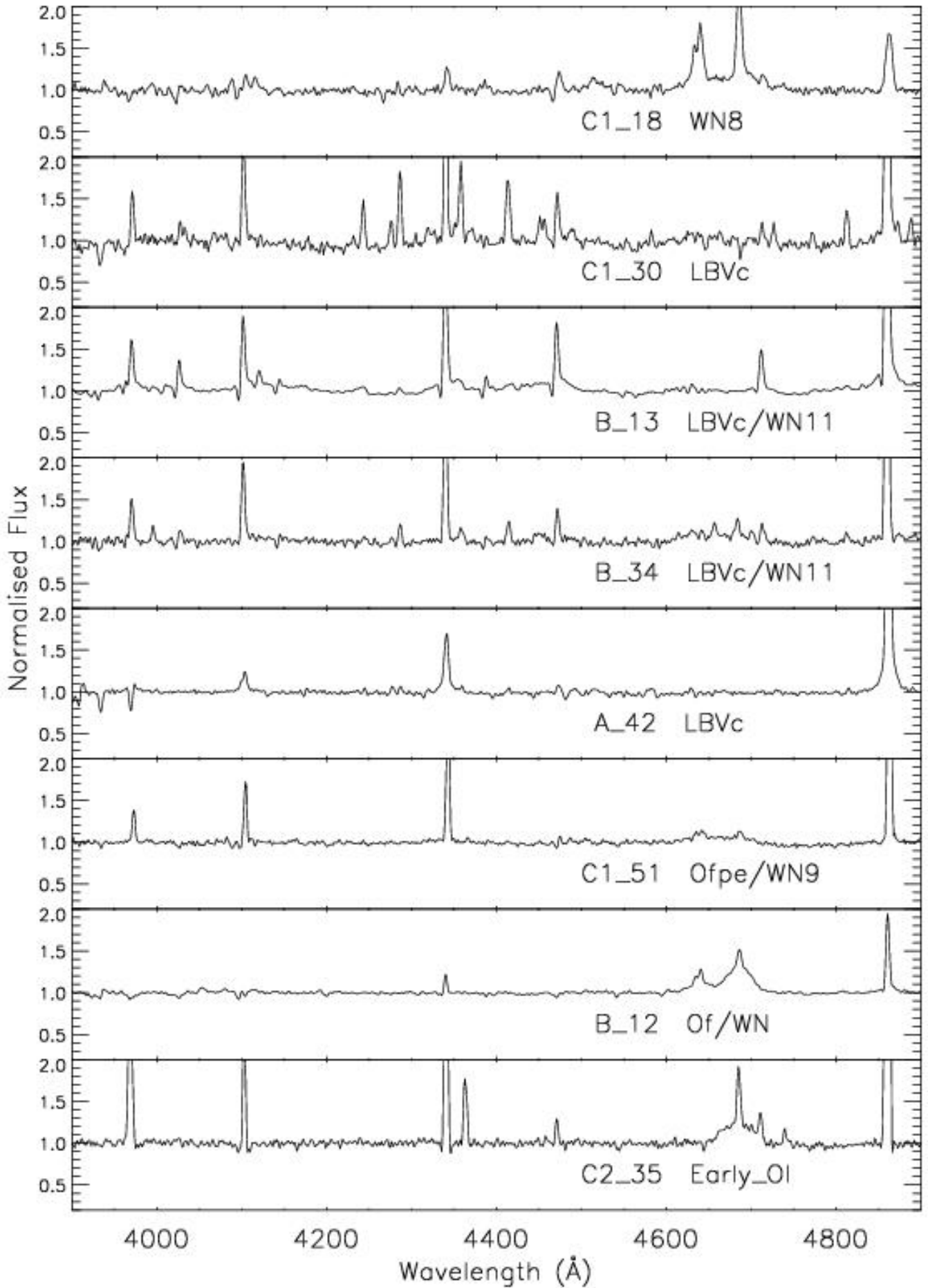
**Table A.2.** F- and G-type stars observed in NGC 55. Columns are detailed in Table A.1.

ID	RA(J2000)	DEC(J2000)	V	V-I	Spectral Type	R <sub>g</sub>	$v_r$	S/N	Metallicity	Comments
(1)	(2)	(3)	(4)	(5)	(6)	(7)	(8)	(9)	(10)	(11)
D_2	0:14:11.65	-39:08:19.69	20.461	-0.213	F0-2I	-634.56	17	36	-	
D_33	0:14:32.48	-39:11:11.40	17.808	-0.223	F5I	-317.28	56	166	-	neb.
D_34	0:14:33.65	-39:10:56.64	19.475	-0.051	F5I	-300.21	30	46	-	neb.
D_41	0:14:39.70	-39:10:56.64	18.418	-0.024	F5-8I	-210.06	55	76	-	
C2_6	0:14:41.86	-39:12:40.68	19.545	-0.088	F2-5I	-178.08	69	68	-	
C1_2	0:14:42.13	-39:10:51.96	18.887	-0.383	F0-2I	-174.36	126	64	-	
D_44	0:14:42.61	-39:10:39.01	19.163	0.253	G0-2I	-168.53	95	25	-	
C2_4	0:14:43.18	-39:11:11.04	19.666	-0.387	F0-2I	-157.39	87	39	-	neb.
C1_6	0:14:45.67	-39:11:14.64	17.392	-0.077	G0I	-120.14	69	104	-	
C2_9	0:14:45.99	-39:11:51.72	19.459	-0.265	F2-5I	-114.18	126	30	-	
C1_12	0:14:50.42	-39:11:09.25	18.345	-0.329	F5-8I	-52.05	133	107	-	neb.
C1_25	0:14:56.02	-39:12:14.39	17.310	-0.287	F8I	39.24	92	109	-	neb.
C2_30	0:14:56.08	-39:12:50.40	19.480	-0.517	F0-2I	51.00	141	32	-	neb.
C1_28	0:14:57.43	-39:12:33.13	17.611	-0.410	F5I	62.83	189	158	-	neb.
C2_31	0:14:59.10	-39:11:37.32	18.107	-0.282	F8I	82.76	123	114	-	
C1_29	0:14:59.39	-39:11:49.19	18.230	-0.342	F8I	86.90	143	88	-	
B_4	0:15:10.36	-39:12:27.36	17.987	0.328	G0-2I	252.59	177	101	-	neb.
B_5	0:15:11.07	-39:12:54.71	18.759	0.134	F8I	265.17	164	76	-	neb.
B_6	0:15:11.58	-39:13:06.24	19.402	0.123	G0I	273.91	176	48	-	neb.
C1_50	0:15:12.90	-39:13:27.48	17.635	-0.006	F5-8I	295.94	138	162	-	
C2_52	0:15:13.51	-39:12:52.92	18.064	-0.261	F5I	301.29	204	87	-	
C2_53	0:15:13.88	-39:13:04.08	18.737	-0.102	F5I	307.78	189	81	-	
B_10	0:15:13.88	-39:13:41.87	19.274	0.180	F8I	312.24	179	57	-	neb.

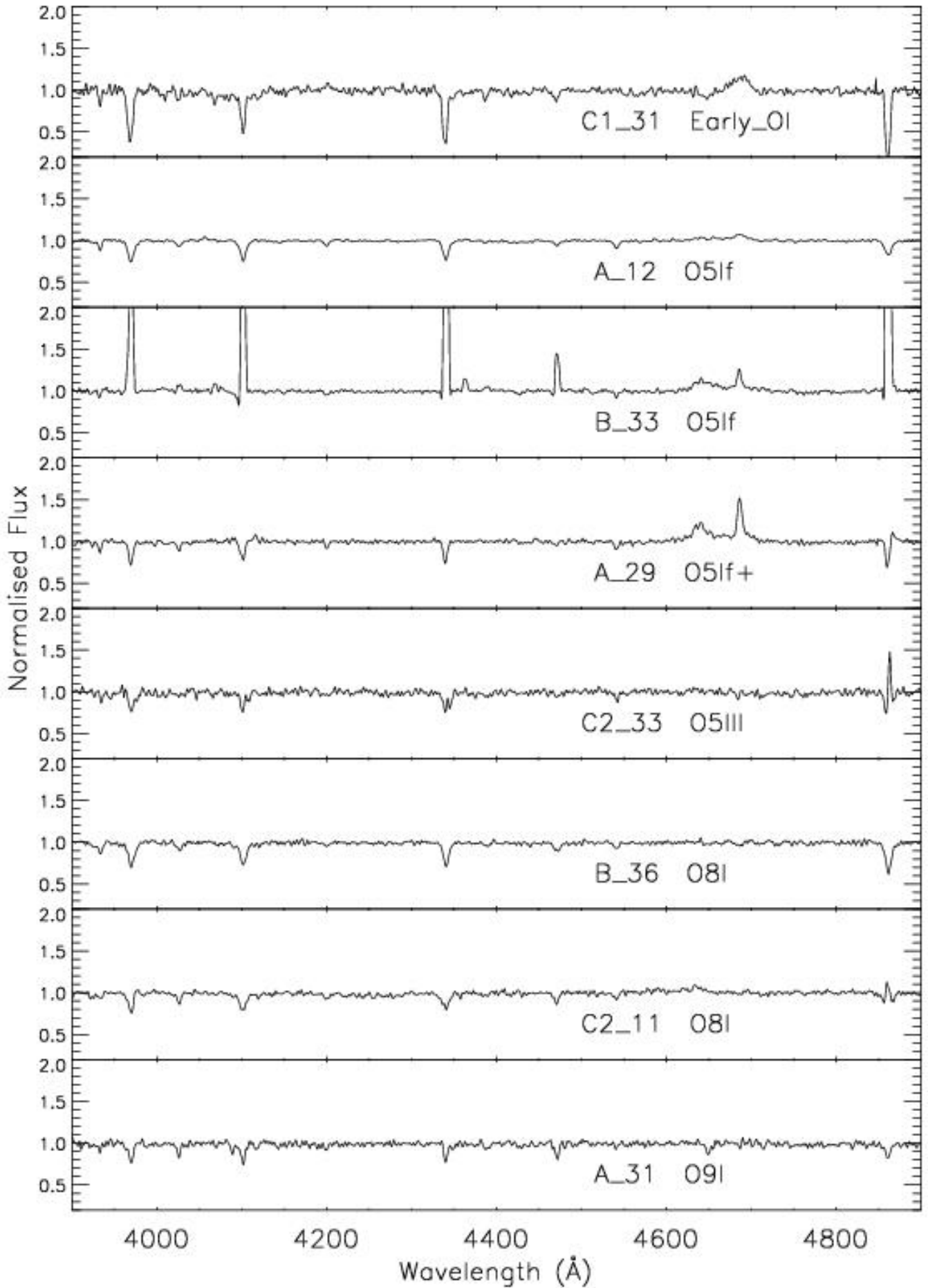
**Table A.3.** Low luminosity class stars, likely members of the Milky Way halo. Columns are the same as in Table A.1.

ID (1)	RA(J2000) (2)	DEC(J2000) (3)	V (4)	V-I (5)	Spectral Type (6)	R <sub>g</sub> (7)	$v_r$ (8)	S/N (9)	Metallicity (10)	Comments (11)
D_8	0:14:16.16	-39:09:38.16	18.945	-0.161	A5V	-564.09	75	69	-	neb.
D_30	0:14:32.02	-39:10:17.03	19.746	0.139	G2-5V	-326.59	34	36	-	
C1_3	0:14:40.77	-39:12:01.07	19.016	-1.017	Da	-192.58	106	111	-	
C2_3	0:14:42.07	-39:11:17.16	19.045	-0.020	B2V	-173.70	107	40	-	
C1_7	0:14:45.26	-39:11:42.36	18.455	-0.197	G0-2V	-125.18	136	93	-	neb.
C2_7	0:14:45.38	-39:11:17.16	18.440	-0.160	B3V	-124.34	79	55	-	neb.
C1_26	0:14:55.76	-39:12:36.72	19.046	-0.388	B8V	42.26	171	40	-	neb.
C1_33	0:15:03.24	-39:11:52.08	17.373	-0.056	G5V	144.62	74	131	-	
B_1	0:15:11.68	-39:10:10.57	18.120	0.191	G0-2V	277.62	160	117	-	
B_14	0:15:21.01	-39:12:50.05	19.677	0.006	B2V	413.07	179	75	-	neb.
B_27	0:15:28.60	-39:13:20.64	19.278	-0.014	A5V	528.55	228	43	-	
B_29	0:15:32.54	-39:12:52.56	19.572	0.326	F8V	585.76	157	55	-	
B_32	0:15:38.10	-39:12:08.64	18.438	0.212	G5V	667.73	20	67	-	

## Appendix B: Atlas



**Fig. B.1.** Digital spectral atlas of VLT-FORS2 observations of NGC 55. LBV candidates (LBVc), WRs and Of-stars.

**Fig. B.2.** O-type supergiants in NGC 55.

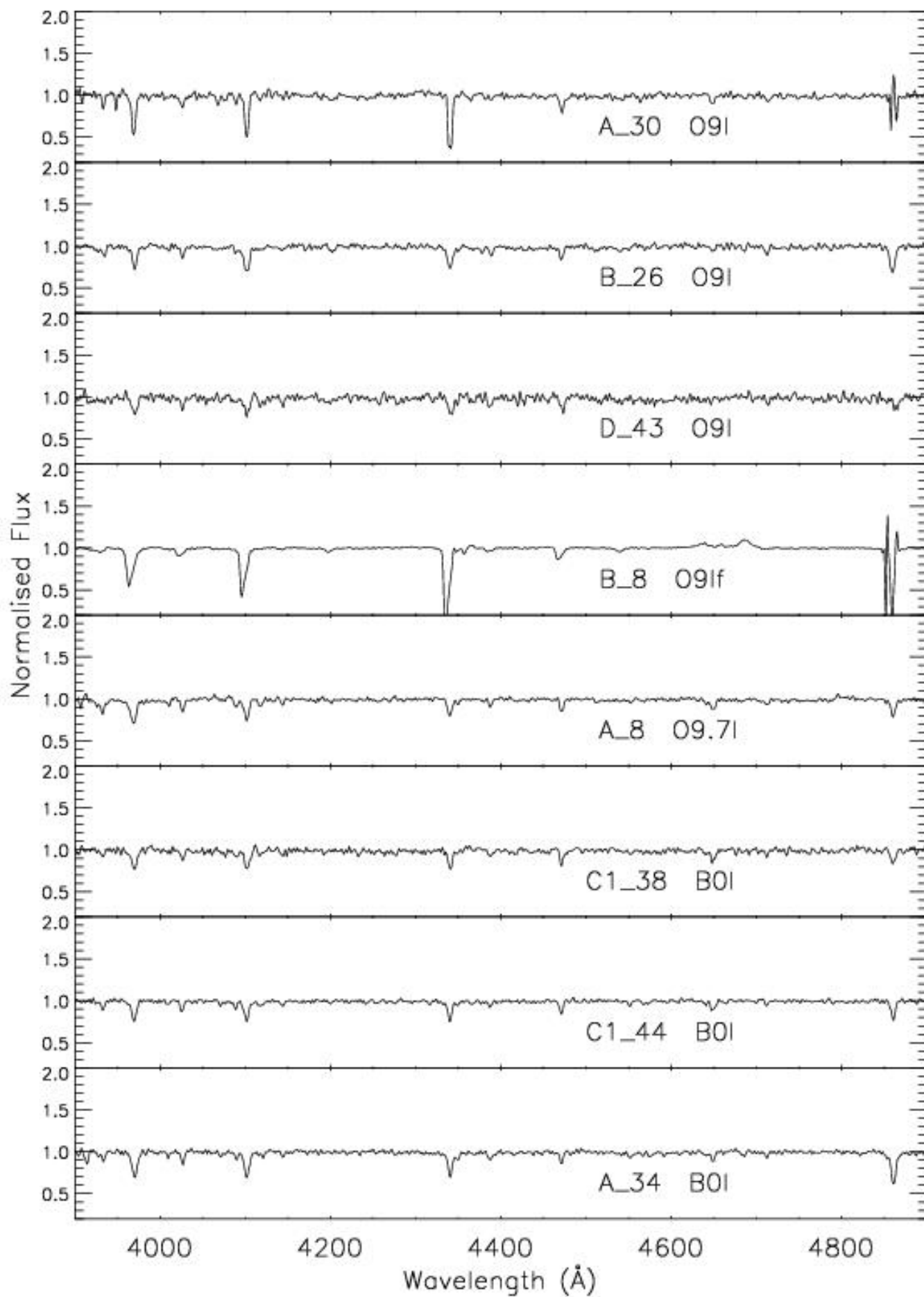
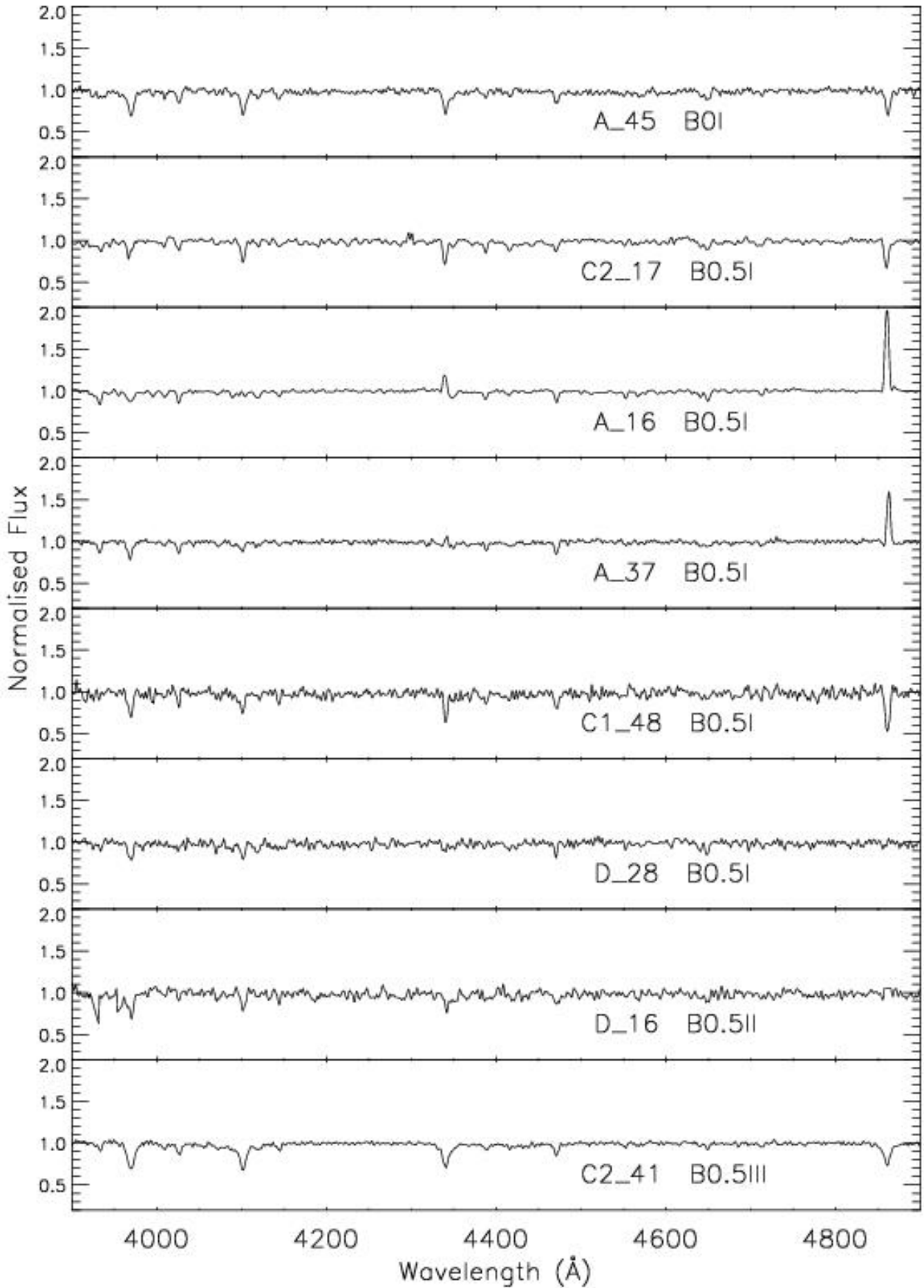


Fig. B.3. Late-O and B0 supergiants in NGC 55.

**Fig. B.4.** B0 stars in NGC 55.

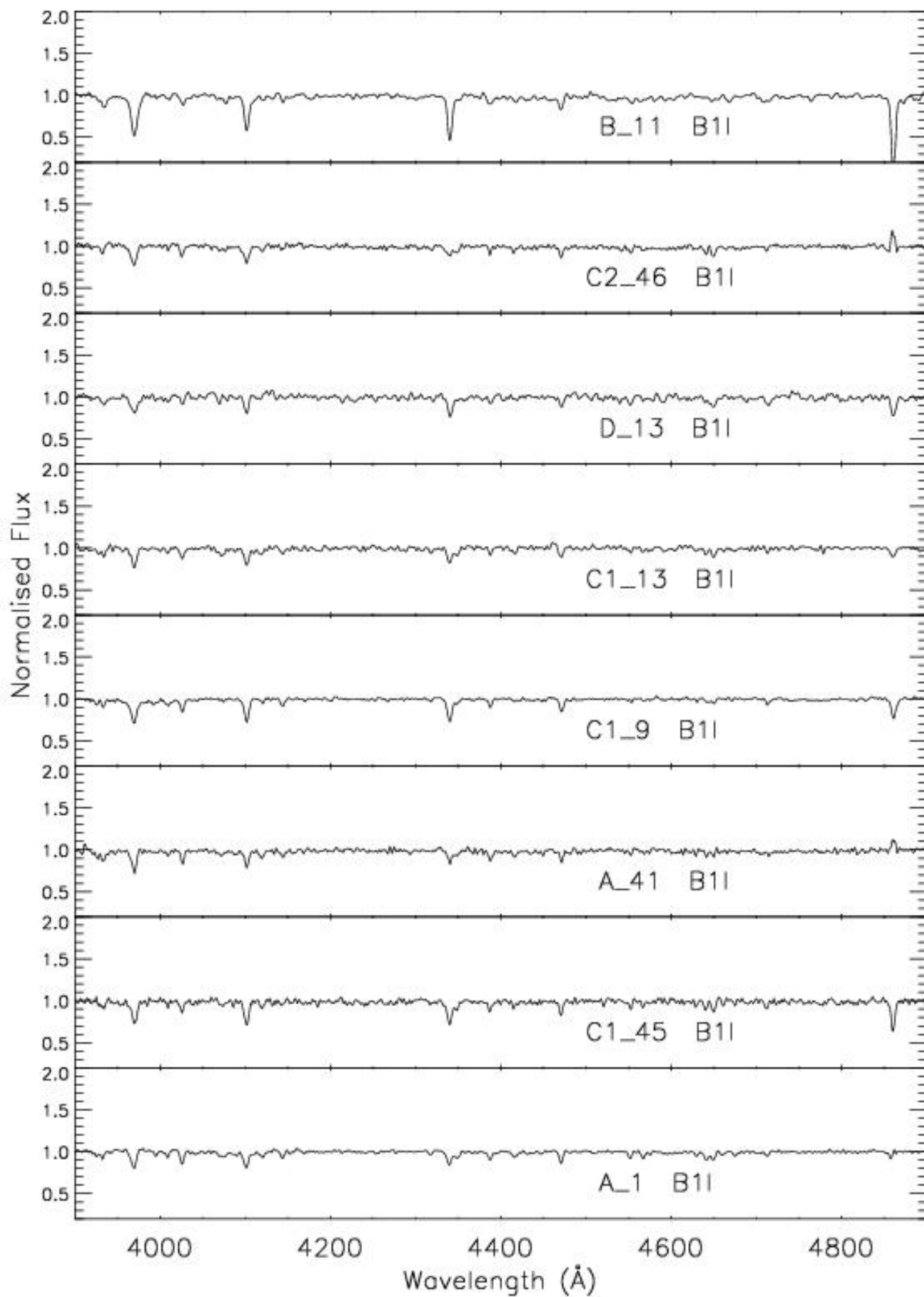


Fig. B.5. B1 supergiants in NGC 55.

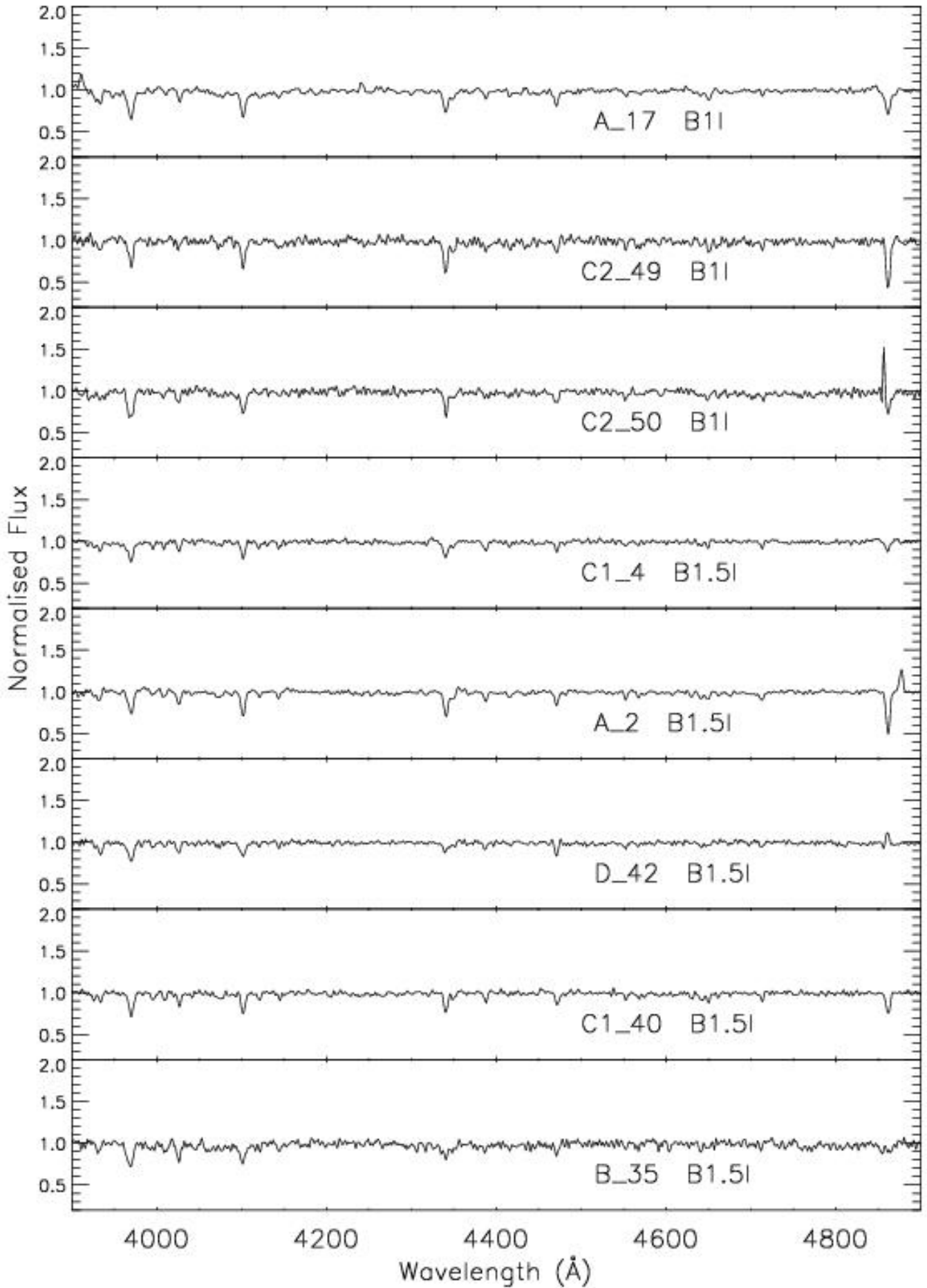


Fig. B.6. B1 supergiants in NGC 55, continued.

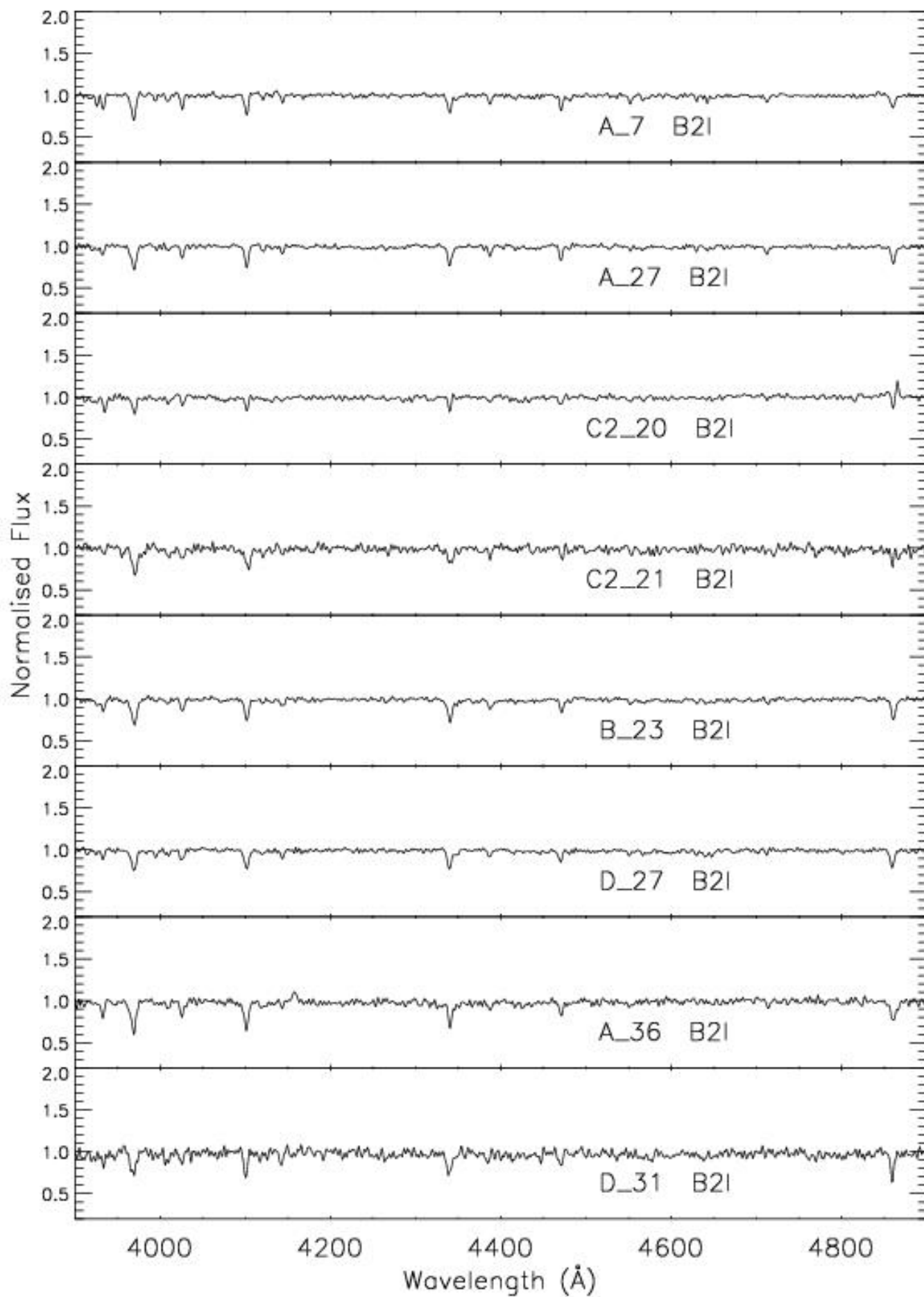
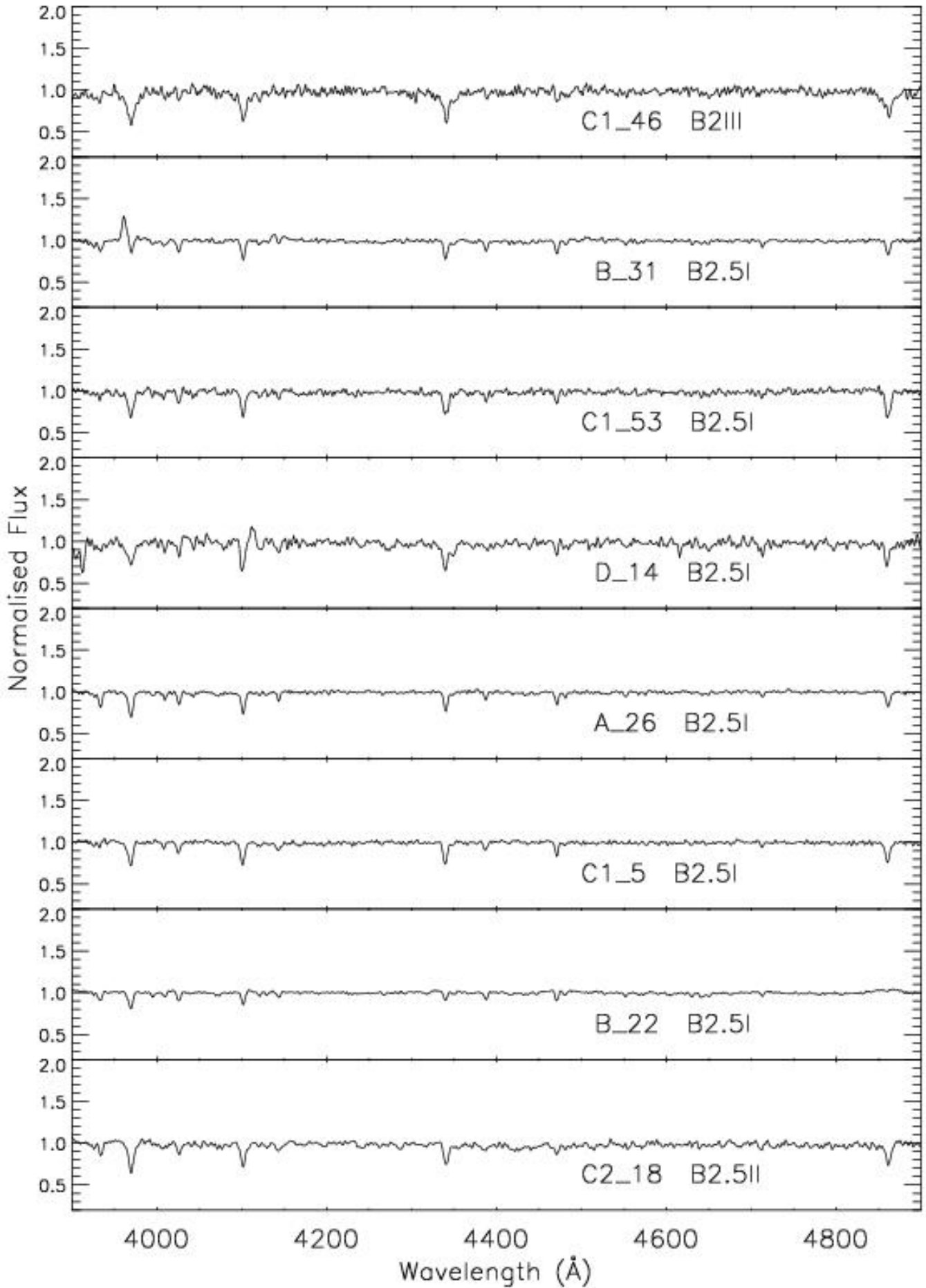


Fig. B.7. B2 supergiants in NGC 55.

**Fig. B.8.** B2 supergiants in NGC 55, continued.

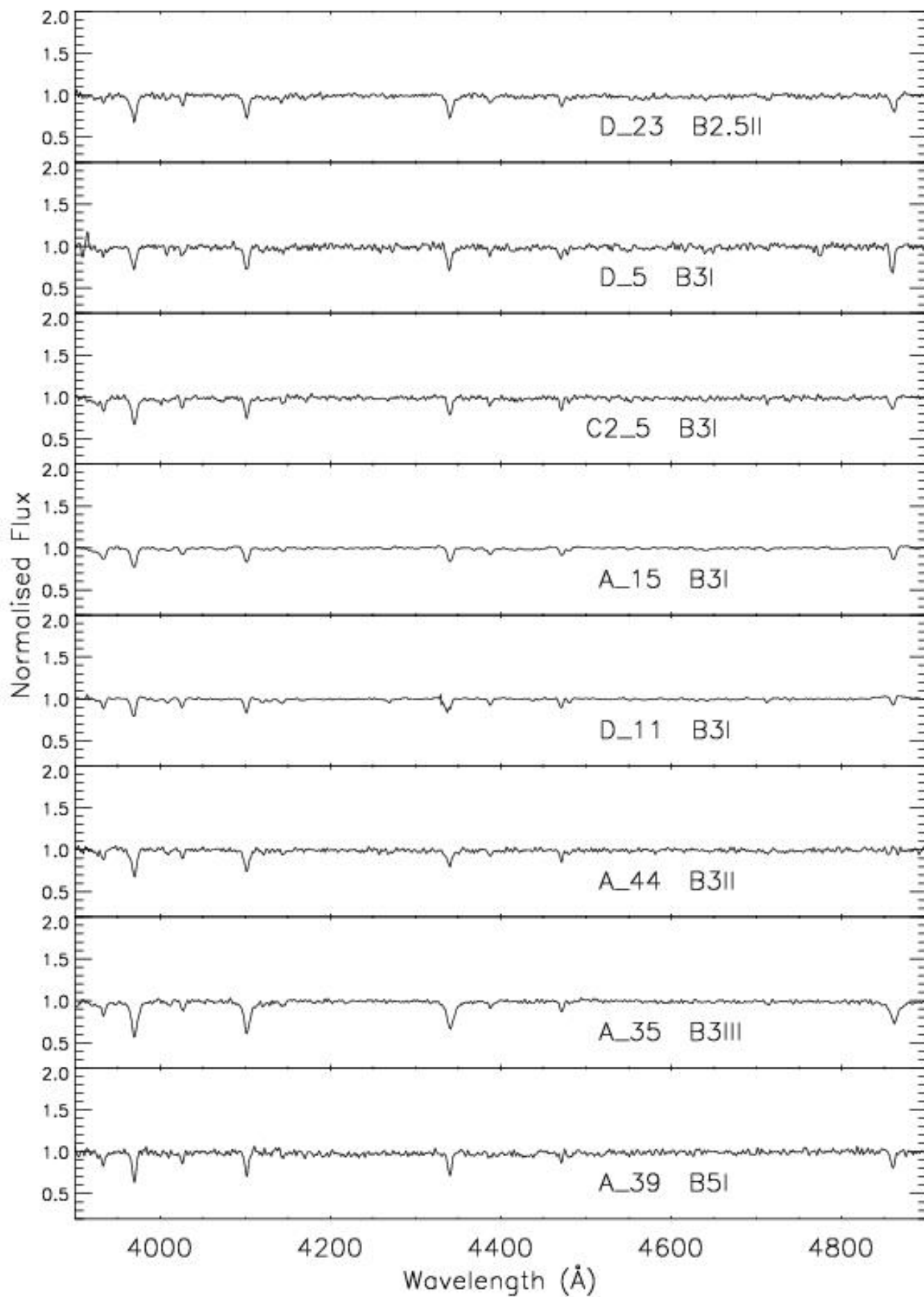


Fig. B.9. Mid-B stars in NGC 55.

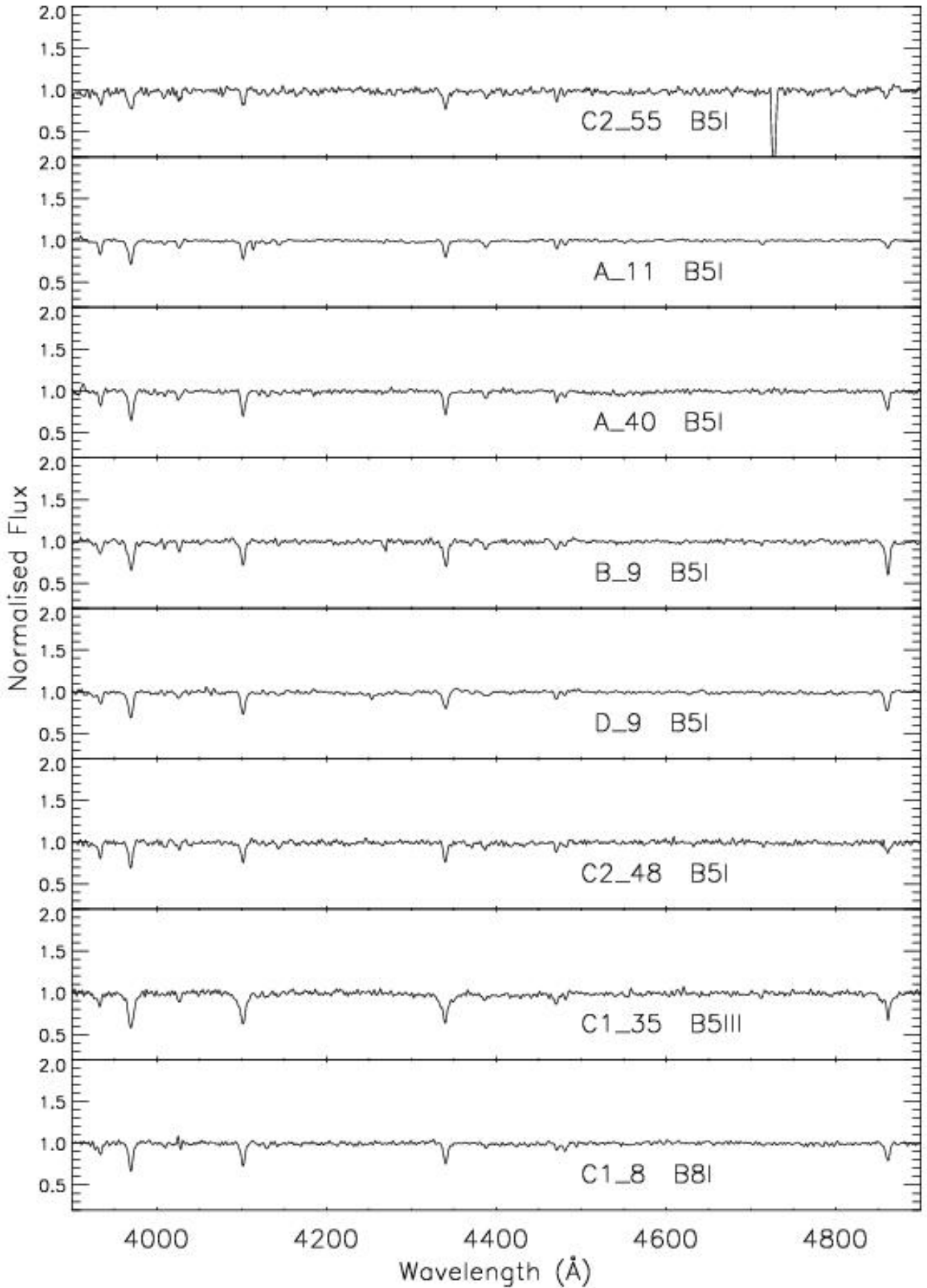


Fig. B.10. Mid-B stars in NGC 55, continued.

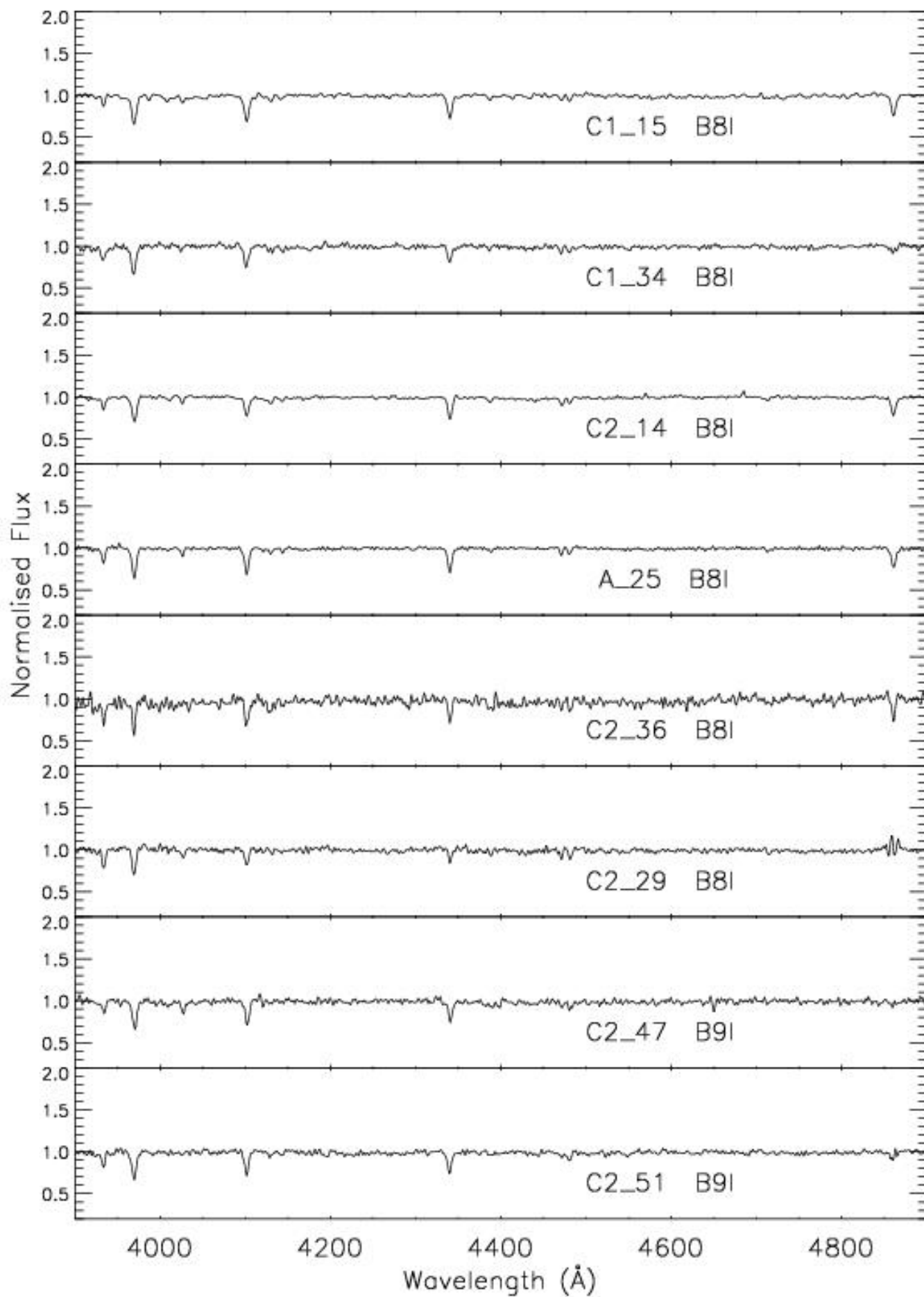


Fig. B.11. Late-B supergiants in NGC 55.

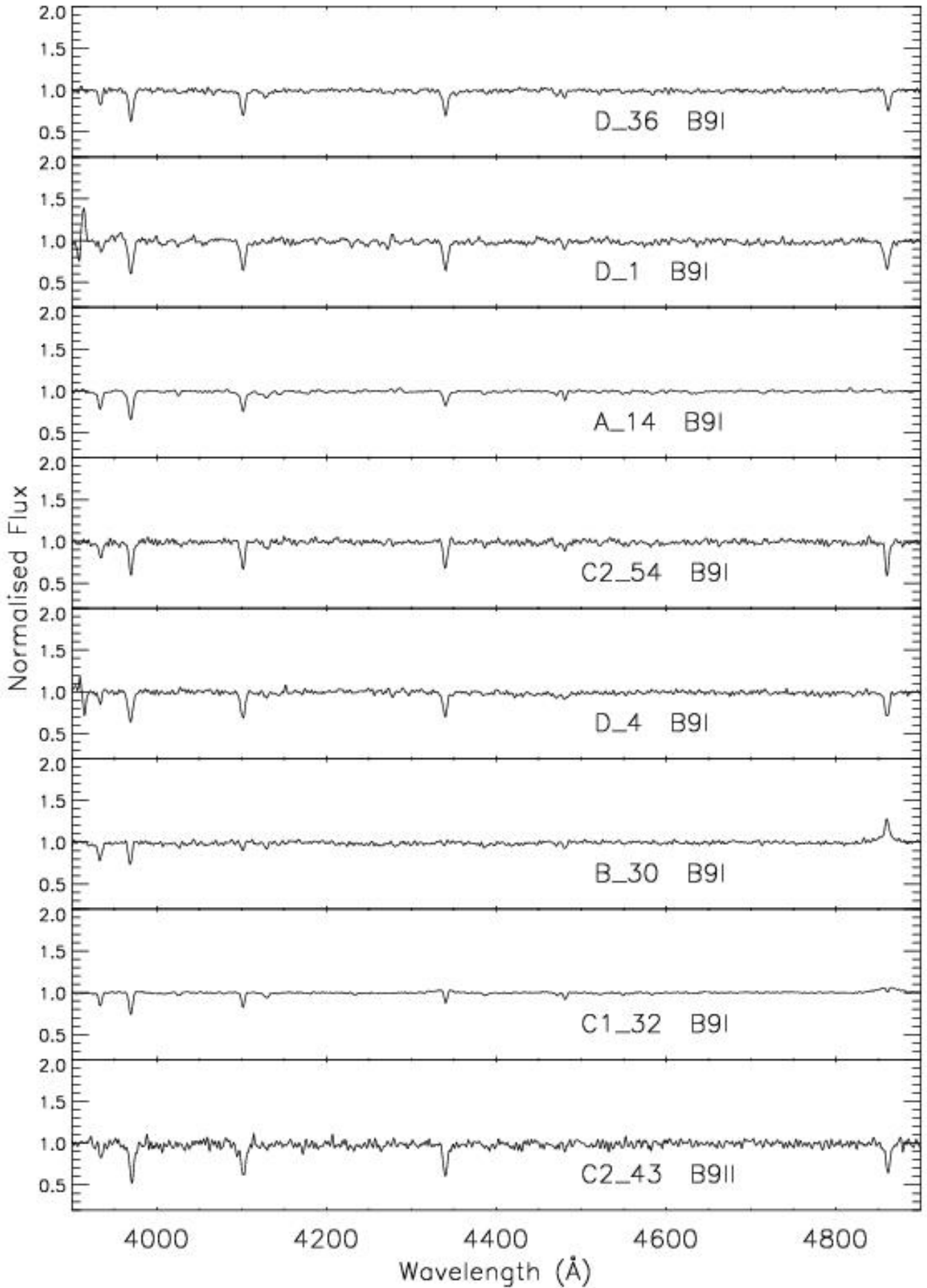


Fig. B.12. Late-B supergiants in NGC 55, continued.

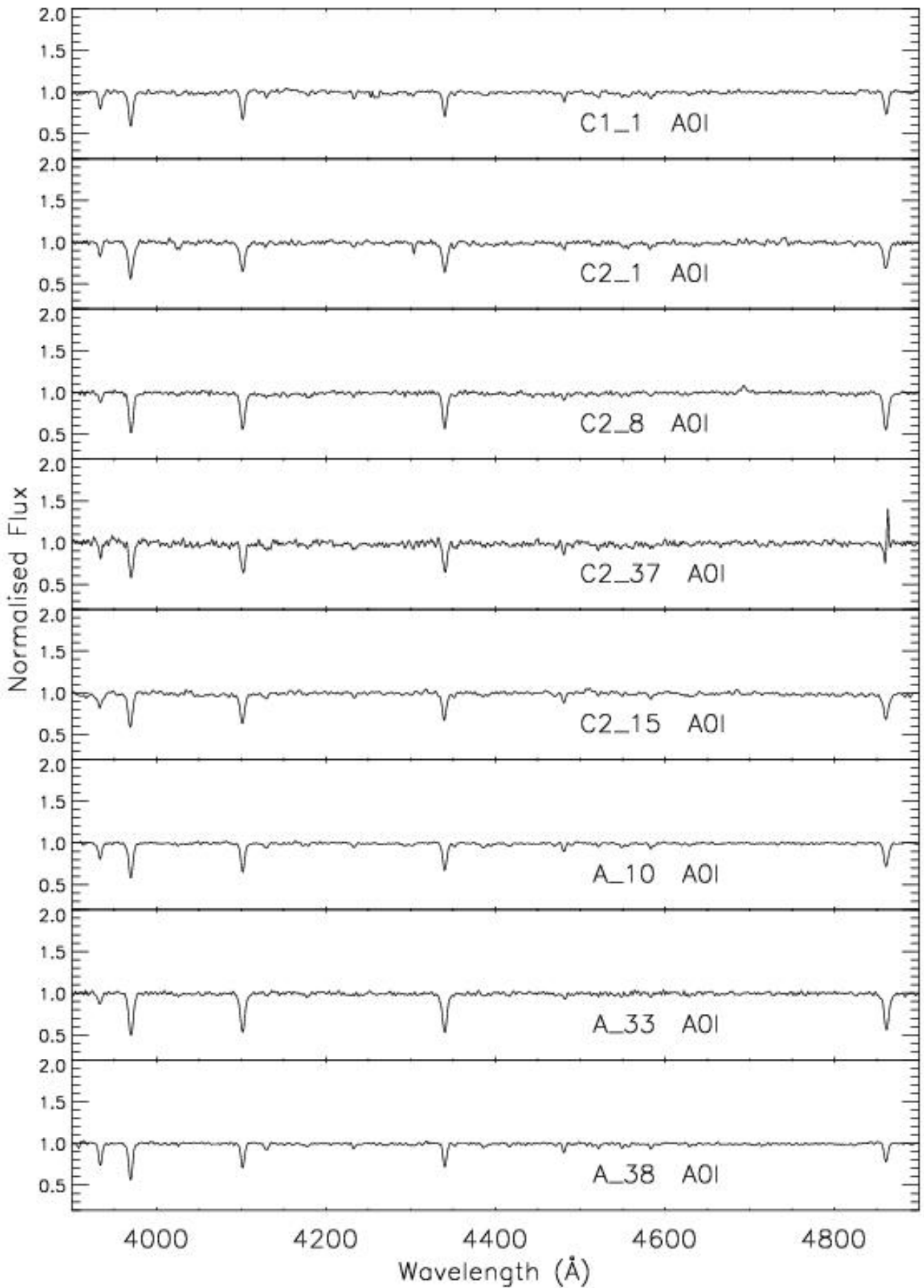


Fig. B.13. A0 supergiants in NGC 55.

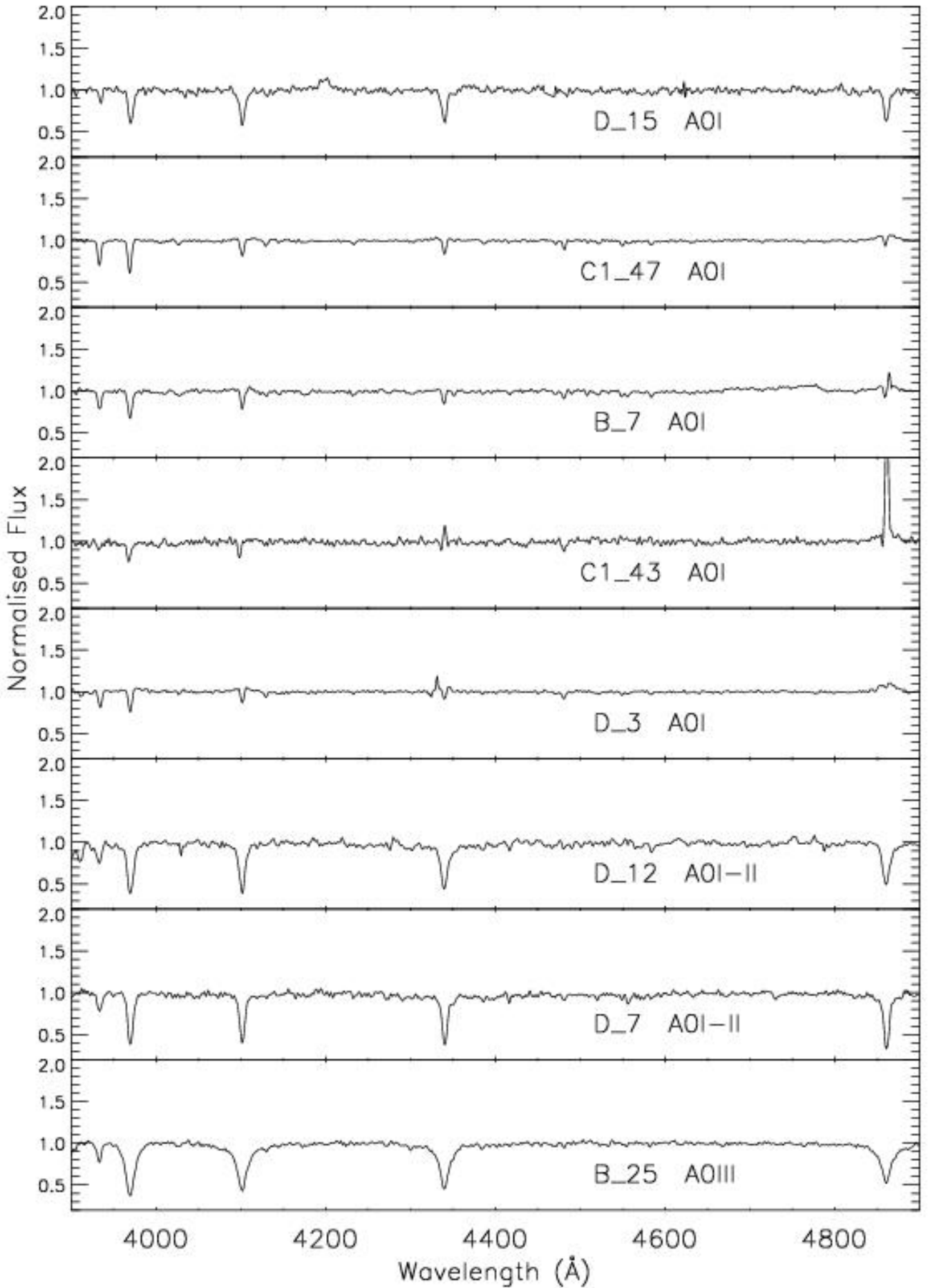


Fig. B.14. A0 stars in NGC 55, continued.

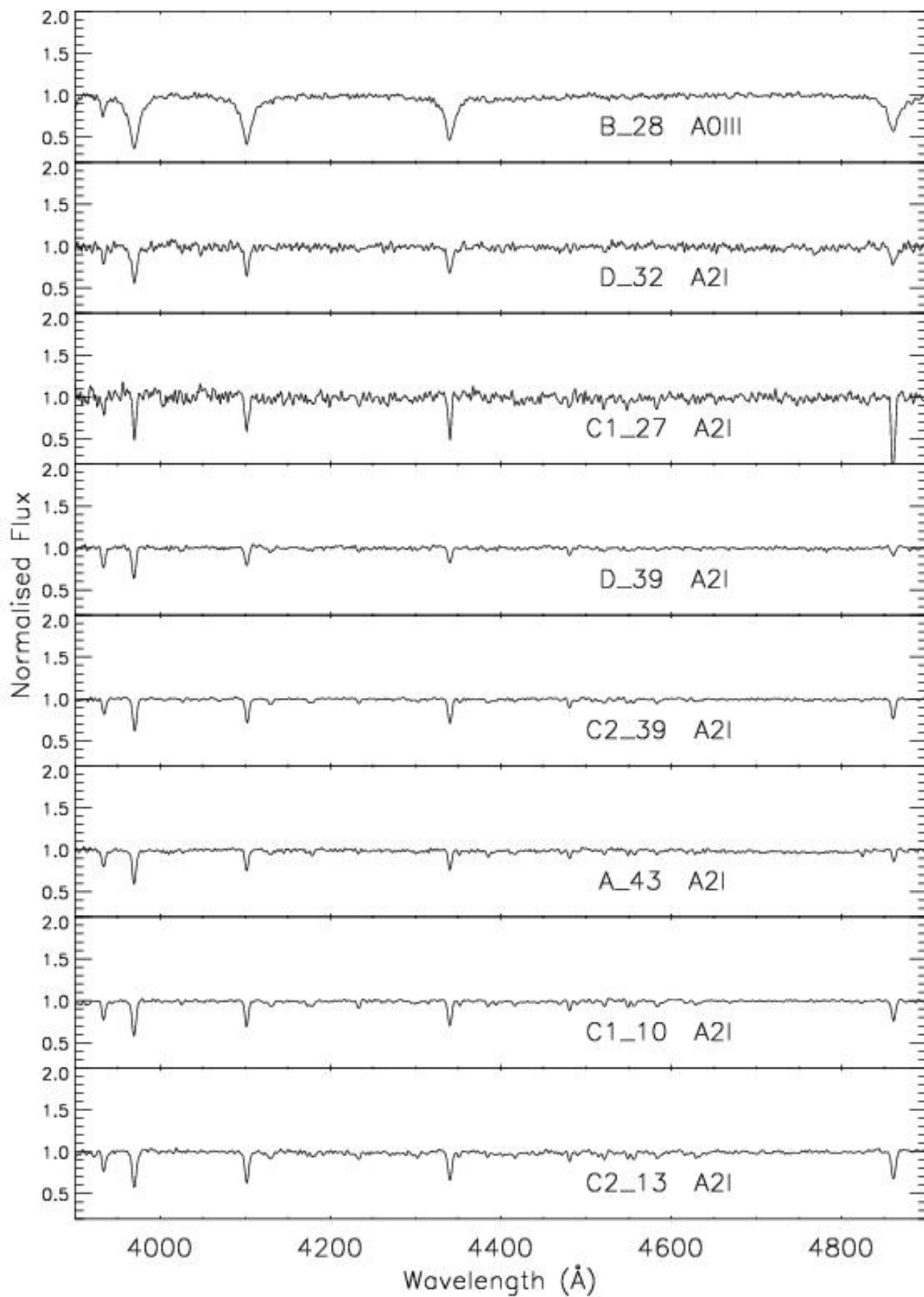


Fig. B.15. Early-A stars in NGC 55.

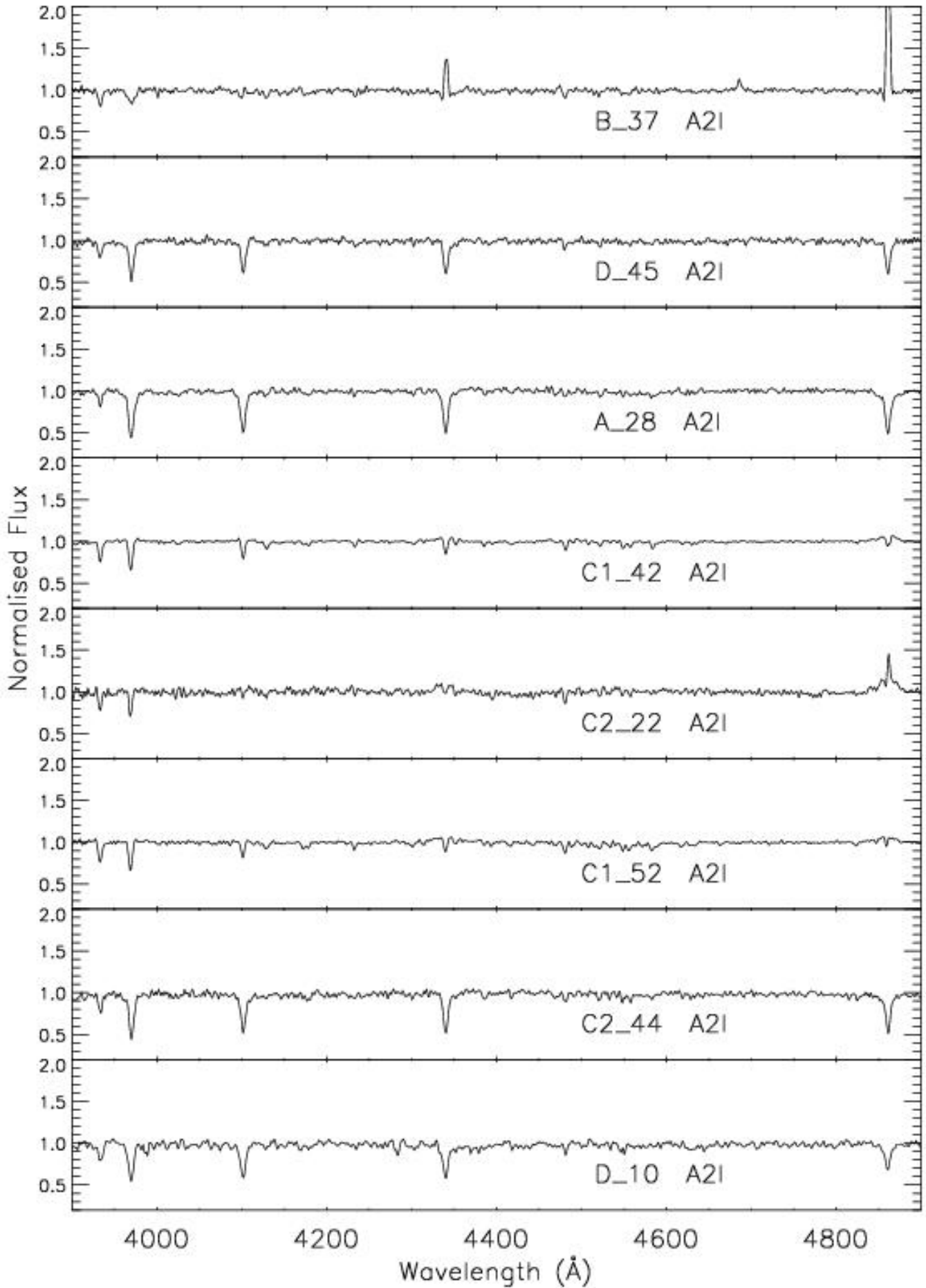


Fig. B.16. A2 supergiants in NGC 55.

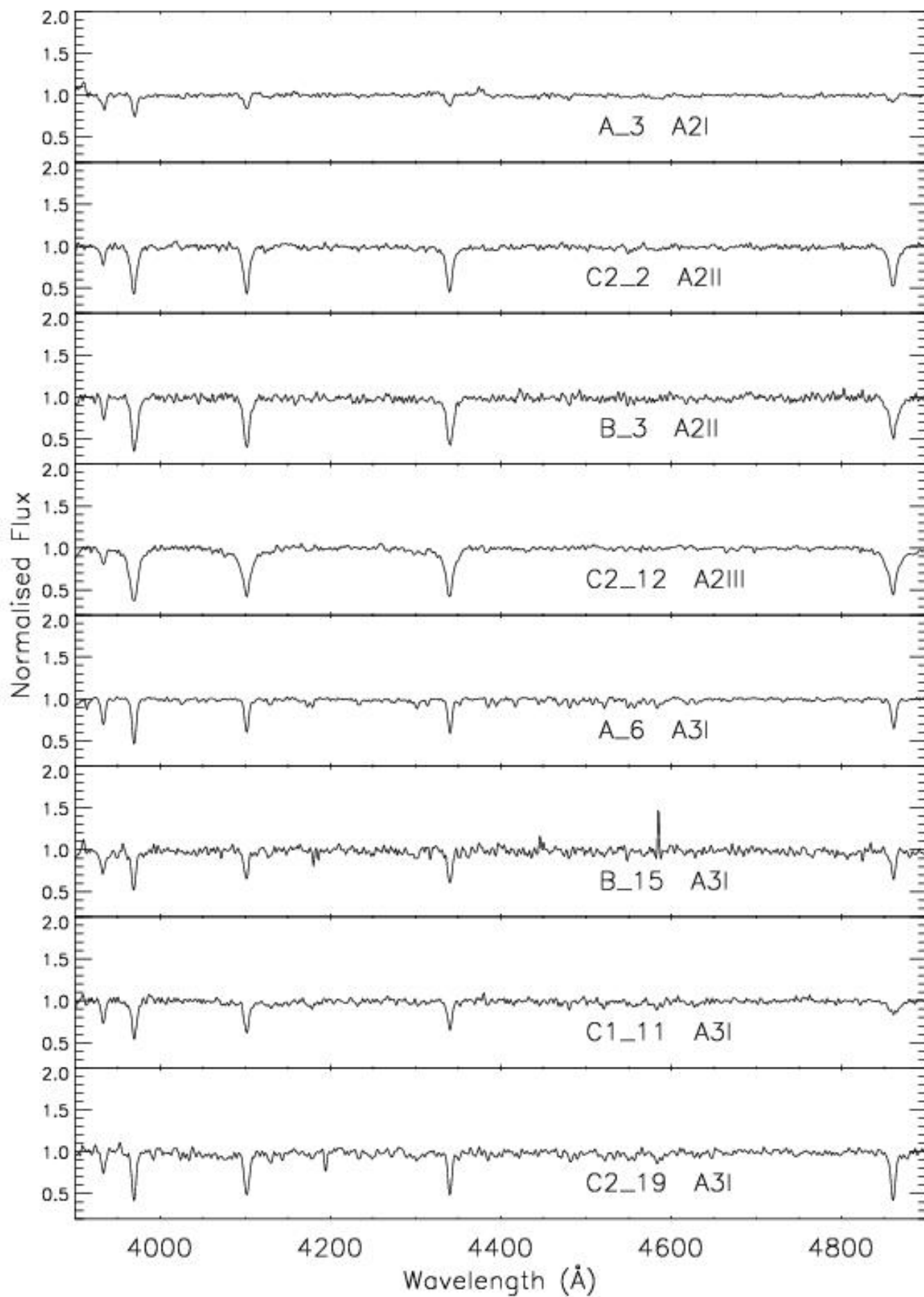


Fig. B.17. A2 and A3 stars in NGC 55.

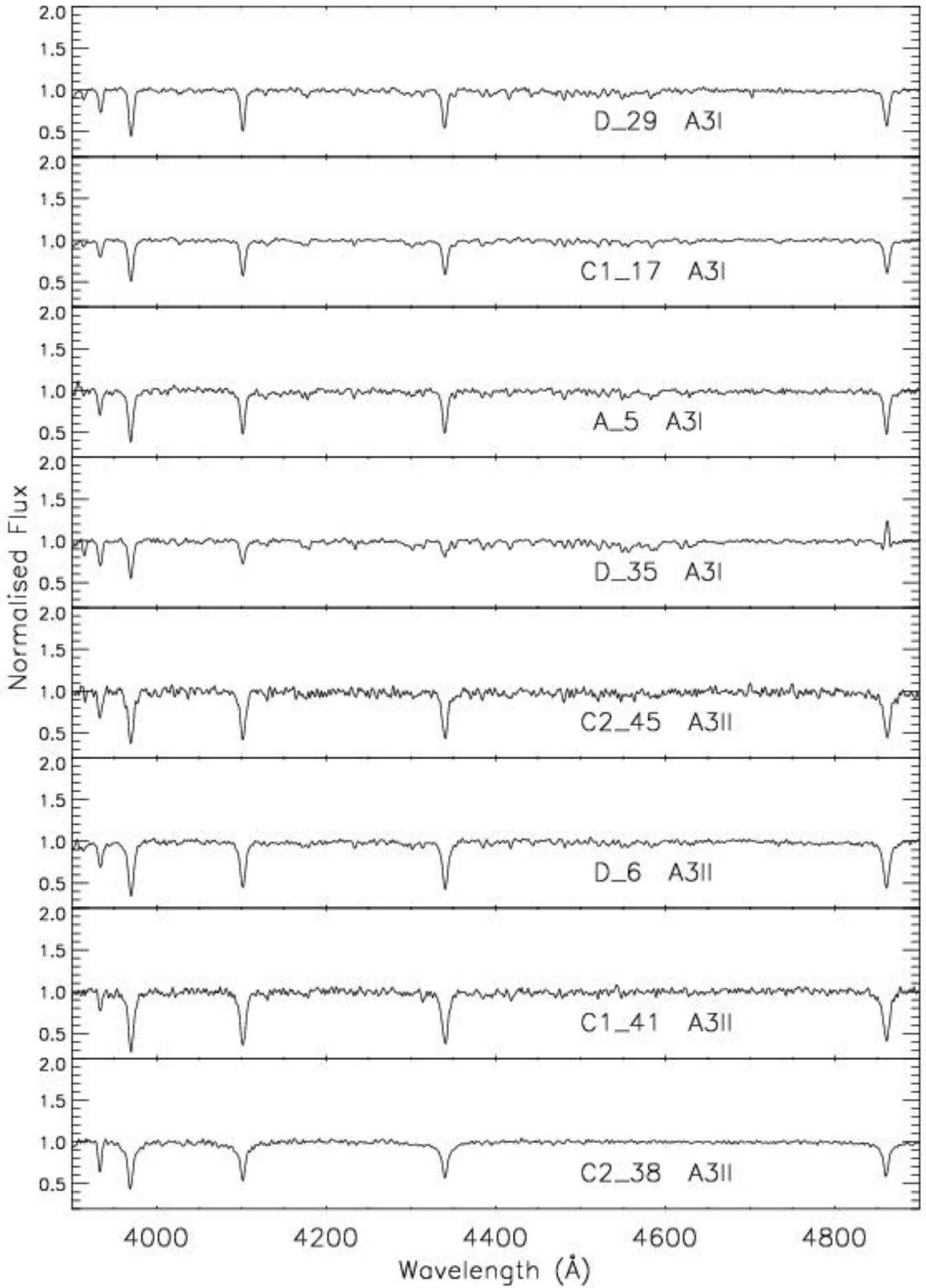


Fig. B.18. A3 stars in NGC 55.

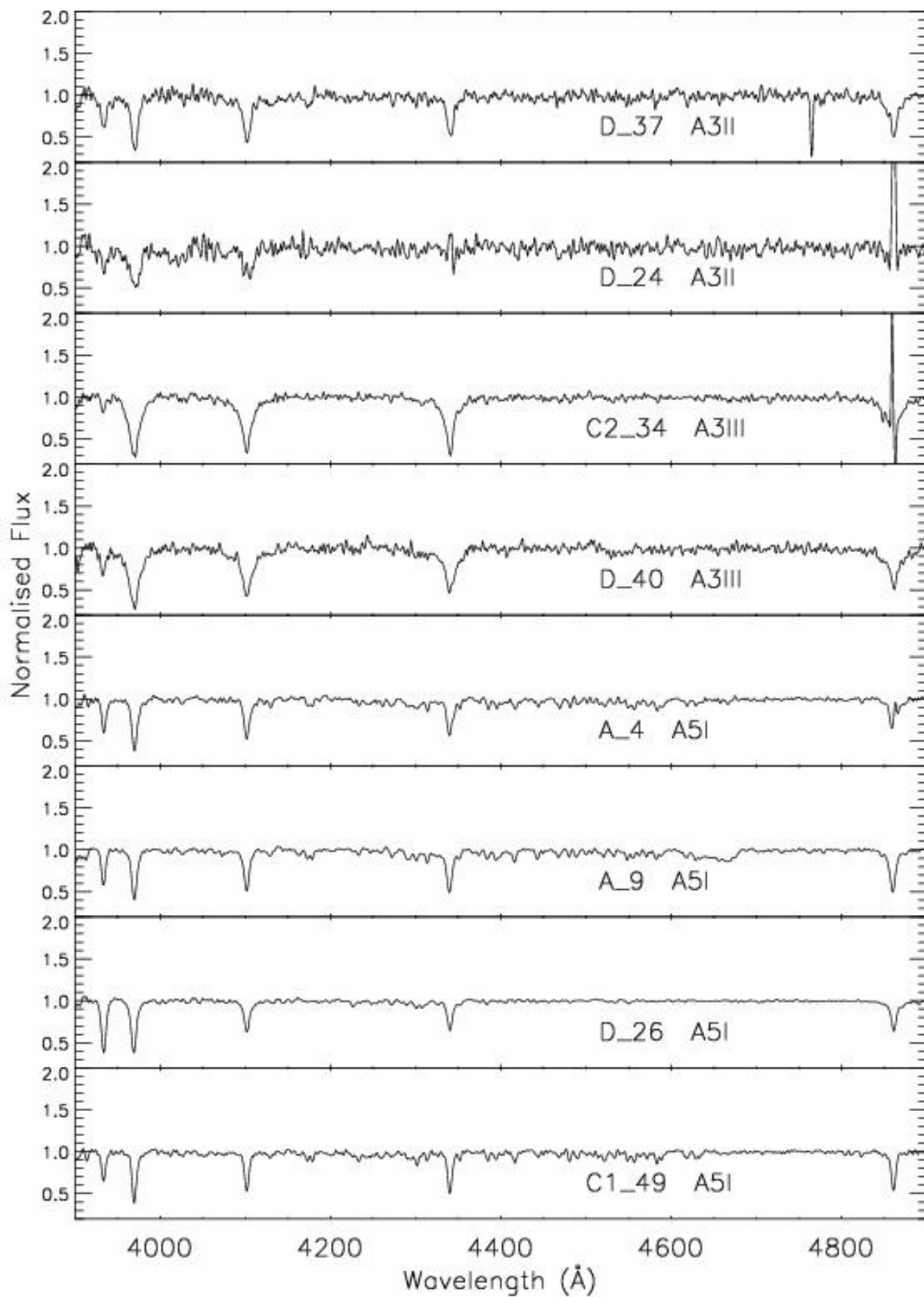


Fig. B.19. Mid-A stars in NGC 55.

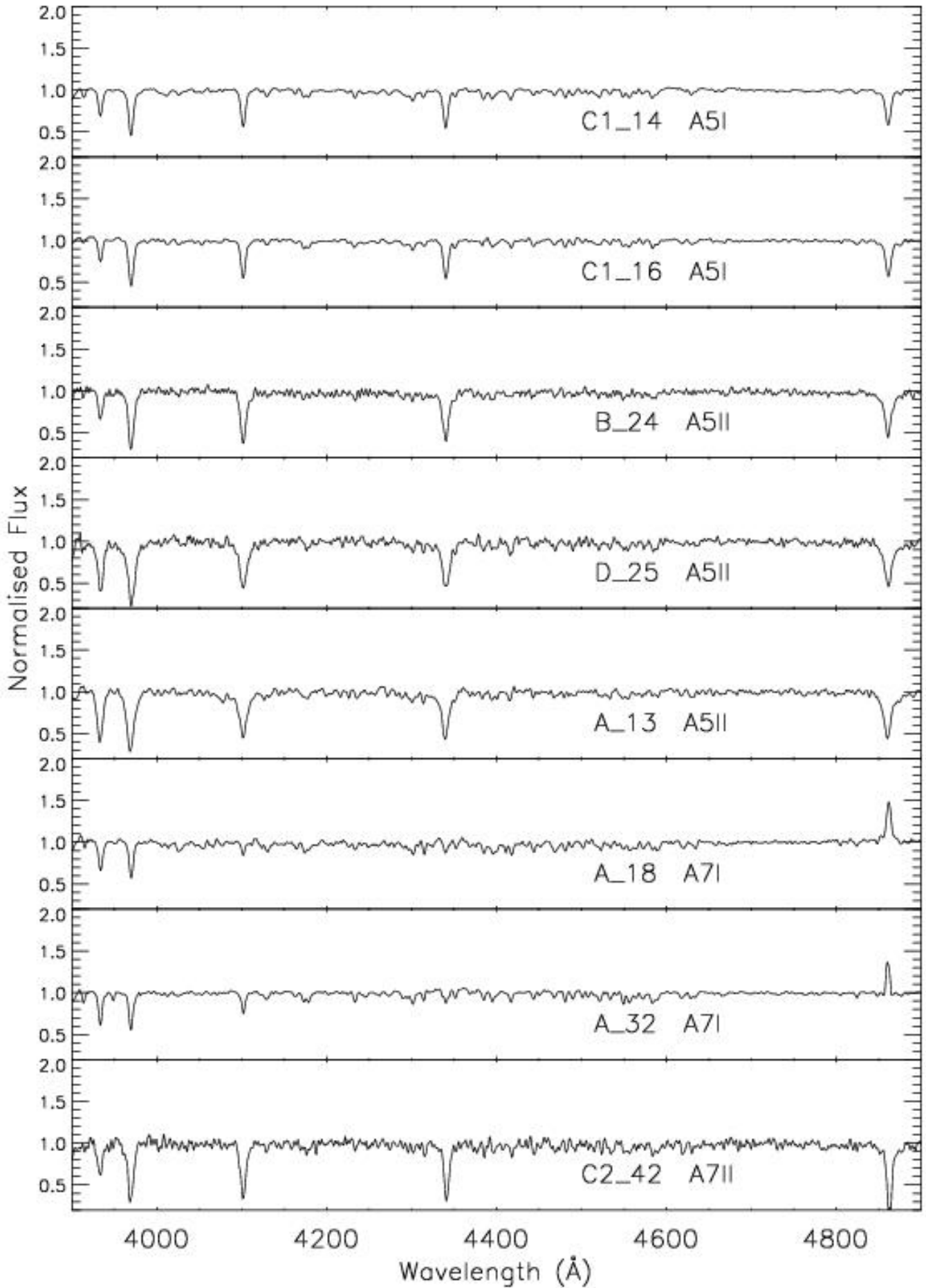


Fig. B.20. Late-A stars in NGC 55.

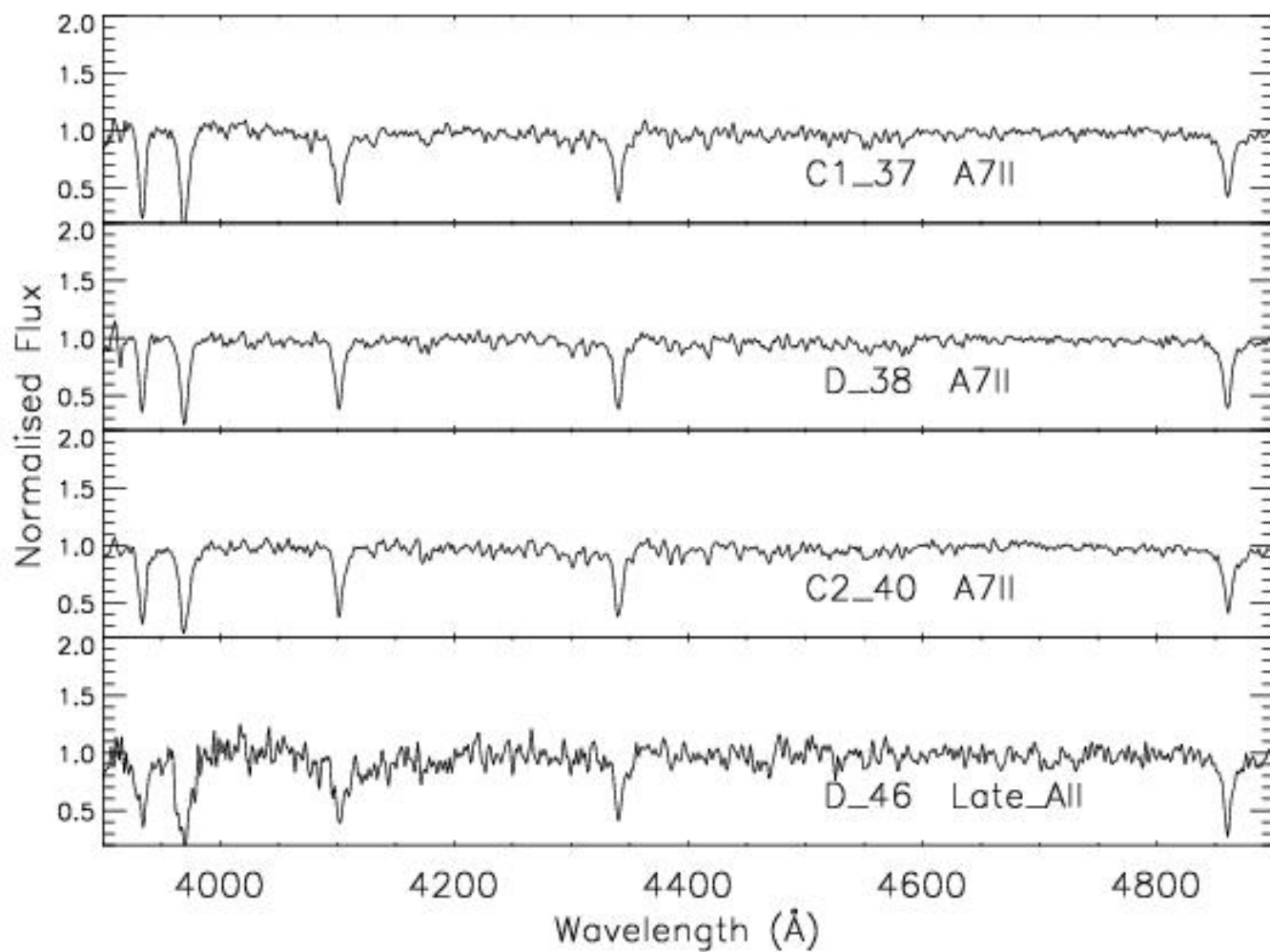


Fig. B.21. Late-A stars in NGC 55, continued.

## Appendix C: Finding Charts

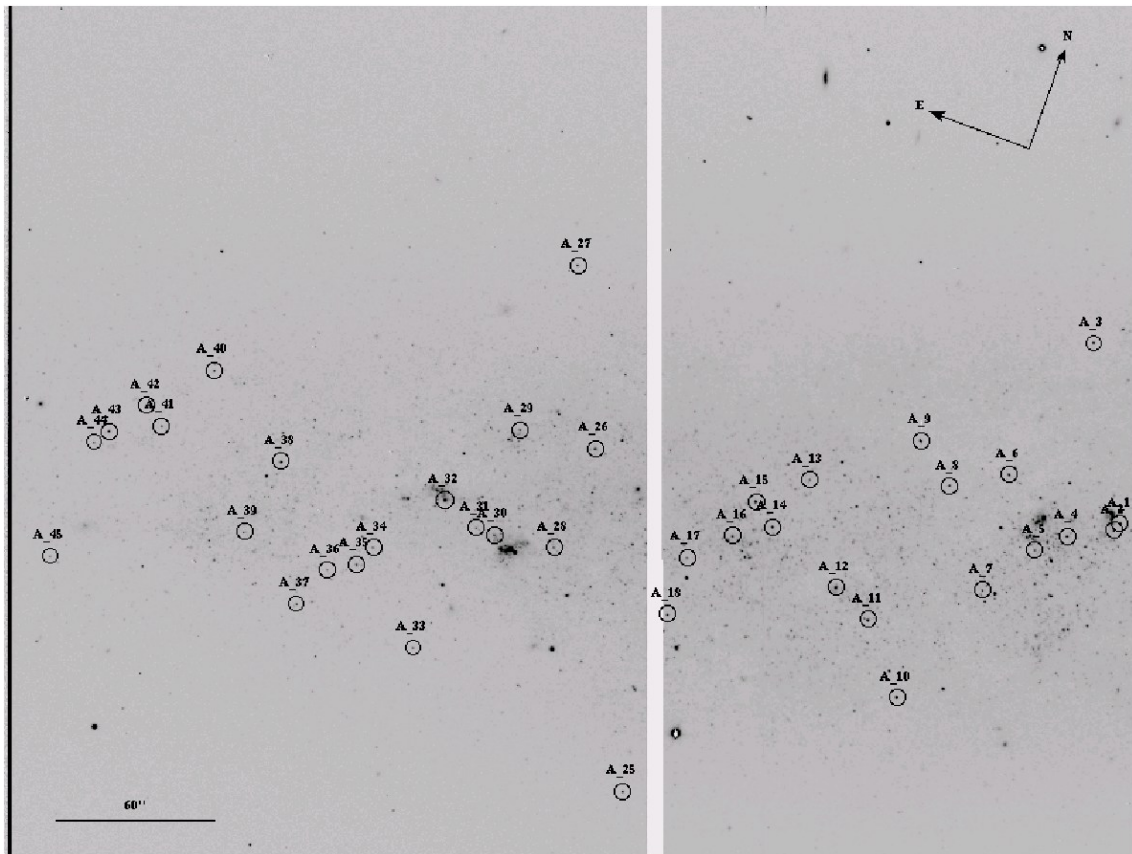


Fig. C.1. FORS2 V-band preimaging of field A. The stars studied in this work are labelled and encircled.

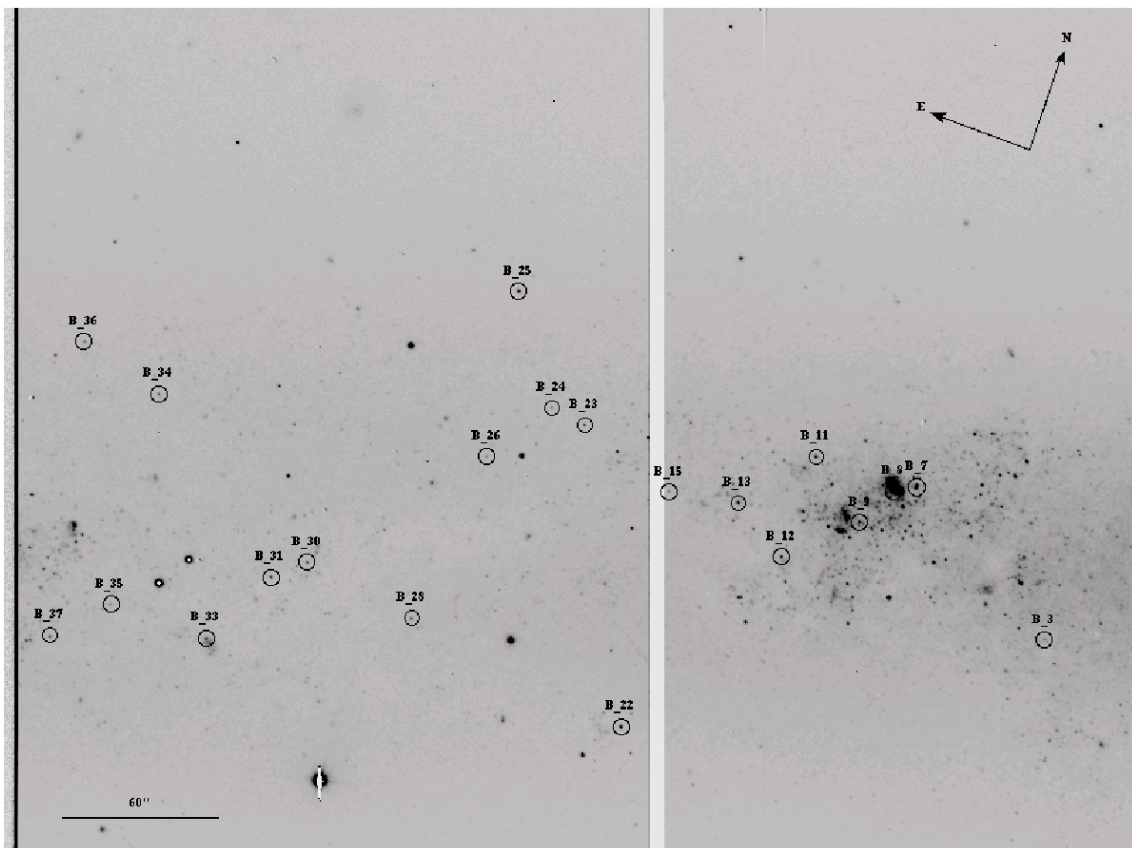


Fig. C.2. Same as Fig. C.1. Target stars in field B.

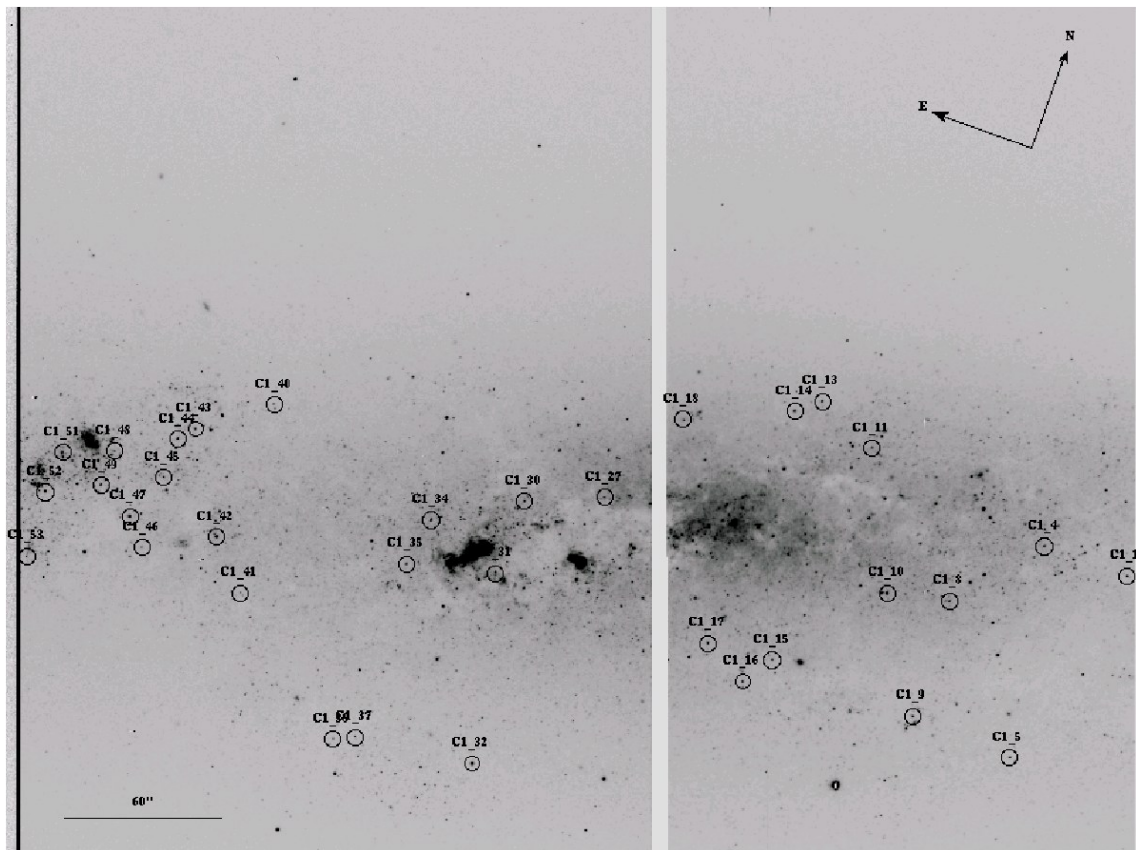


Fig. C.3. Same as Fig. C.1. Target stars in field C observed through mask C1.

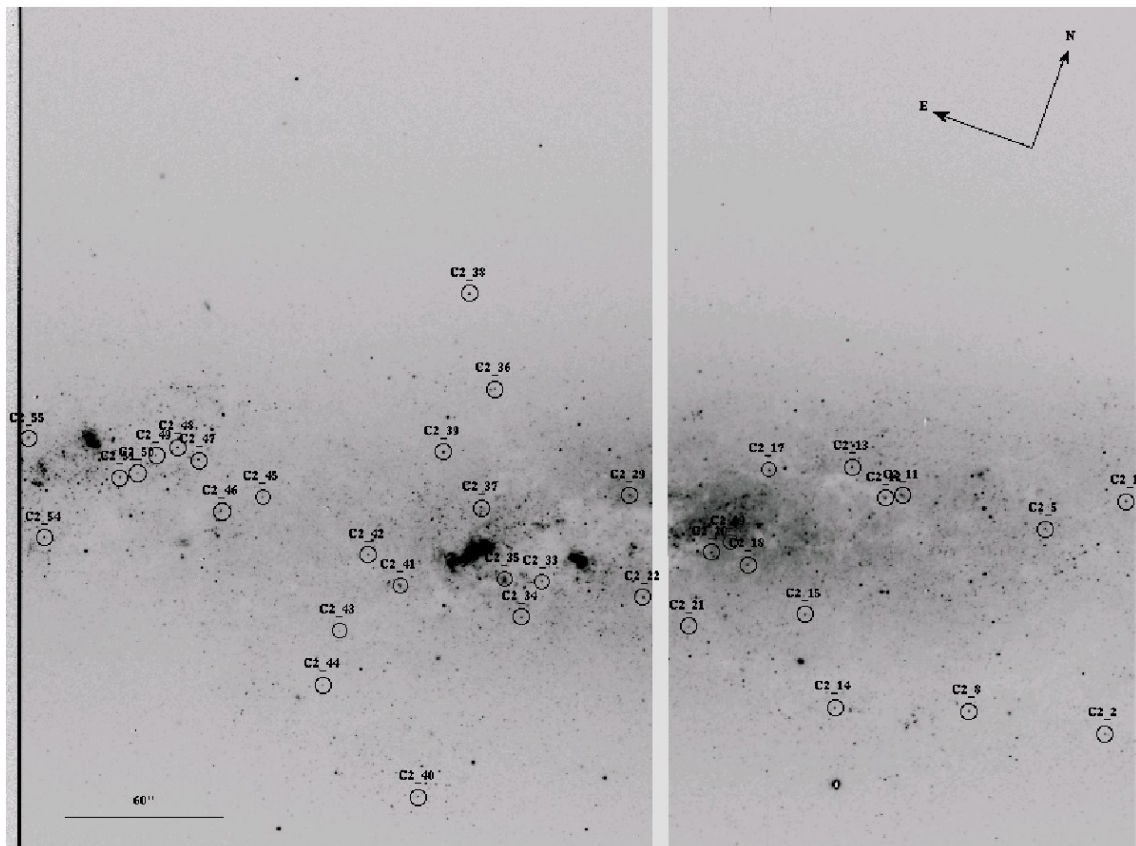


Fig. C.4. Same as Fig. C.1. Target stars in field C observed through mask C2.

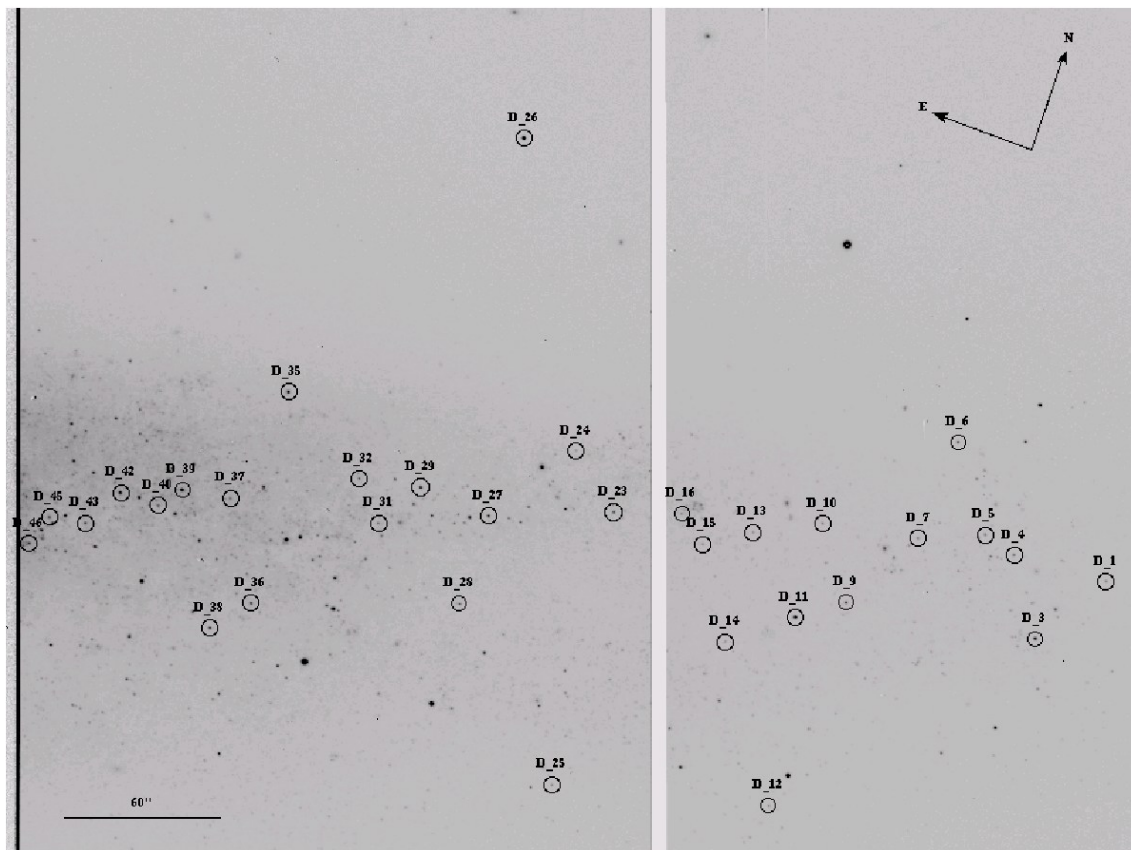


Fig. C.5. Same as Fig. C.1. Target stars in field D.